CHAOS IN ORIENTATION REVERSING TWIST MAPS OF THE PLANE

J.B. van den Berg, R.C. Vandervorst, and W. Wójcik

Abstract. We study forcing of periodic points in orientation reversing twist maps. First, we observe that the fourth iterate of an orientation reversing twist map can be expressed as the composition of four orientation preserving positive twist maps. We then reformulate the problem in terms of parabolic flows, which form the natural dynamics on a certain space of braid diagrams. Second, we focus our attention on period-4 points, which we classify in terms of their corresponding braid diagrams. They can be categorized in two types. If an orientation reversing twist map has a period-4 point of one type, then there is a semi-conjugacy to symbolic dynamics and the system is forced to be chaotic. We also show that this result is sharp in the sense that the remaining type does not necessarily lead to chaos.

1. Introduction

Orientation preserving twist maps have been studied by many authors over the past decades. In particular we mention the important contributions by Moser [**22, 23**], Mather [**20**], Aubry & Le Daeron [**4**], Angenent [**1, 2**], Boyland [**8**] and Le Calvez [**10**]. Most of these works consider area and orientation preserving twist maps and make use of the variational principle that comes with it. This is a powerful tool for studying periodic points, in particular when the domain of the map is an annulus.

In this paper we are interested in dynamical systems generated by *orientation reversing* twist maps that do not necessarily preserve area and that are defined on the whole plane. Specifically, we are interested in periodic orbits and the minimal dynamics they force. We

JB is supported in part by NWO VENI grant 639.031.204 and RCV and WW are supported in part by NWO VIDI grant 639.032.202. This research is also partially supported by the RTN project Fronts-Singularities HPRN-CT-2002-00274, August 3, 2004.

postpone a discussion of related work to the end of this introductory section. First, we give the necessary definitions and introduce a topological principle for such orientation reversing maps.

A well-known example of a two dimensional orientation reversing twist map is the family of Hénon maps. The discrete time dynamics that are obtained by iterating such maps have emerged as models from various applications in the physical sciences. Orientation *preserving* (twist) maps of (sub-regions of) the plane are often obtained as time-1 maps in non-autonomous Hamiltonian systems in the plane, or as first return maps to a Poincaré section in three dimensional dynamical systems. On the other hand, maps that reverse orientation do not occur as such section maps.

In this paper we are mainly concerned with *diffeomorphisms* of the plane, i.e. bijective C^1 maps.

Definition 1.1. A diffeomorphism $f:\ \mathbb{R}^2 \to \mathbb{R}^2$ is called an *orientation reversing twist diffeomorphism* of the plane if there exist global coordinates $(x,y) \in \mathbb{R}^2$ such that f is given by $(x',y') = f(x,y)$ and satisfies the assumptions: (i) $\det(df) < 0$, and (ii) $\frac{\partial x'}{\partial y} > 0$. Due to the latter condition, which we will refer to as the *twist property*, f is said to have *positive* twist. If the bijectivity assumption is dropped but f is still C^1 and satisfies properties (i) and (ii) then f is called an orientation reversing twist *map*.

In the following, to indicate the coordinate functions x' and y' of f, we use the composition with the orthogonal projections π_x and π_y onto the x- and y-coordinate respectively, i.e. $x' = \pi_x f(x,y)$ and $y' = \pi_y f(x,y)$.

As will be explained in Section 3 (see also [**15**]) (compositions of) orientation preserving (positive) twist maps have a natural topological structure, which is less straightforward in the orientation reversing case. There exists an easy procedure to circumvent this obstacle and find a useful topological tool for orientation reversing twist maps. Note that even powers of f are orientation preserving maps, but compositions of twist maps are in general not twist maps. The second composite iterate f^2 can be written as a composition of two orientation *preserving* twist maps as follows: $f^2 = f_+ \circ f_-$, with $f_+ = f \circ R_x$, and $f_- = R_x \circ f$, where R_x is a linear reflection in the y-axis. The drawback is that f_+ is a positive twist map and

f_- a negative twist map. If we consider the fourth iterate f^4 we have the decomposition

$$f^4 = f_3 \circ f_2 \circ f_1 \circ f_0, \tag{1}$$

where the maps f_i are defined as follows:

$$f_0 = -f_-, \quad f_1 = -f_+ \circ (-\mathrm{id}), \quad f_2 = f_- \circ (-\mathrm{id}), \quad \text{and} \quad f_3 = f_+.$$

One can easily verify that all four maps are orientation preserving maps with *positive* twist. The theory of parabolic recurrence relations in [**15**] (summarized in Section 3) is now applicable since it applies to compositions of orientation preserving positive twist maps. Using this formulation we can study periodic points of period $n = 4k$ (for other periods symmetry requirements could be imposed, but we will not pursue this issue here).

Recall that a point $z = (x, y)$ is a period-n point for f if $f^n(z) = z$, where f^n denotes the n-th iterate of f. The period n is assumed to be *minimal*, i.e. $f^k(z) \neq z$ for all $0 < k < n$. Instead of describing a period-4 point in terms of the images of f, i.e. $(z, f(z), f^2(z), f^3(z))$, a natural way to describe orbits is to do so in accordance to the decomposition given by (1). We write an orbit as $\{z_i\}_{i=0}^3$, with $z_i = f_i(z_{i-1})$. This applies to period-$4k$ points, by defining f_i via $f_{i+4} = f_i$, for all $i \in \mathbb{Z}$. The theory of parabolic recurrence relations in [**15**] now dictates that orbits $\{z_i\}$ should be represented as braid diagrams, which we will explain next.

Let z be a period-4 point of f. By choosing the points z, $f(z)$, $f^2(z)$, and $f^3(z)$ as different initial points we obtain four different orbits for the composition $f_3 \circ f_2 \circ f_1 \circ f_0$, namely the orbits defined by $z_i = f_i(z_{i-1})$ while setting $z_0 = f^k(z)$ for $k = 0, 1, 2, 3$. For each orbit we connect the consecutive points (i, z_i) via piecewise linear functions. This yields a piecewise linear closed braid consisting of four strands. By projecting the braid on the x-coordinates one obtains a closed braid diagram. Braid diagrams are discussed in more detail in Section 3.1. Figure 1 depicts the braid diagrams which result from this construction starting from two different period-4 orbits. Since the braid diagram is only concerned with the x-coordinates the construction of the braid diagram is, for all practical purposes, equivalent to the following: let (x^0, x^1, x^2, x^3) be the x-coordinates of a period-4 point orbit $\{f^k(z)\}_{k=0}^3$, i.e. $x^i = \pi_x f^i(z)$, then perform a flip on these coordinates to obtain $(x_0, x_1, x_2, x_3) = (-x^0, x^1, x^2, -x^3)$, and finally connect the points (i, x_i) in the plane by line segments. This gives one strand and the total braid diagram is obtained by performing this transformation to all shifts of the orbit through z.

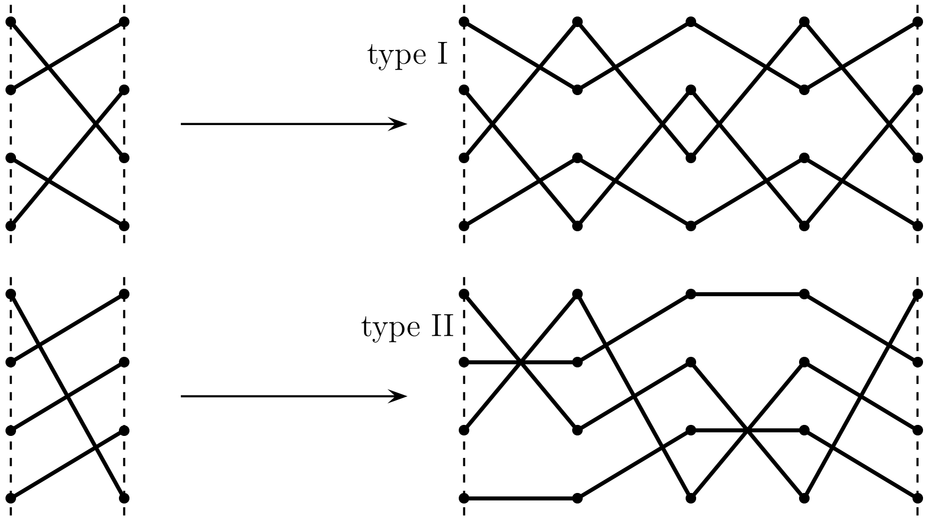

Figure 1. Period-4 points lead to *two* possible braid classes. In the braid diagrams on the right one may think of all the crossings as being positive, i.e. the strand with the larger slope going on top.

Notice that period-4 points can occur in a variety of six different "permutations" (of the x-coordinates, see also Section 4). However, permutations do not have topological meaning with respect to parabolic recurrence relations and permutations are thus not suitable for classifying period-4 points. On the other hand, via the above construction each permutation yields a unique braid class that has a topological meaning. It follows that period-4 points give rise to exactly two types of braid classes. Figure 1 shows the two possible braid classes: type I and type II. In other words, *any* period-4 orbits is either of type I or of type II, according to the braid class that results from the above transformations. More details on this classification are supplied in Section 4. Period-4 points of type I imply chaos, while those of type II do not, as is stated in our main theorem.

Theorem 1.2. *An orientation reversing twist diffeomorphism of the plane that has a type I period-4 point is a chaotic system, i.e., there exists a compact invariant subset* $\Lambda \subset \mathbb{R}^2$ *for which* $f|_\Lambda$ *has positive topological entropy. Conversely, there exists an orientation reversing twist diffeomorphism with a type II period-4 point that has zero entropy.*

We want to point out that the theorem is stated under quite weak assumptions; in particular, there are *no* compactness assumptions (the twist property in a way compensates this lack of compactness). The bijectivity assumption in the theorem is certainly stronger than strictly necessary. In fact, instead, for twist maps it is more natural to assume the infinite twist condition: a twist map is said to satisfy the *infinite twist* condition if

$$\lim_{y\to\pm\infty} \pi_x f(x,y) = \pm\infty \qquad \text{for all } x \in \mathbb{R}. \tag{2}$$

For twist maps on the plane this condition in some sense means that the map has positive twist at infinity (not an infinite amount of twist). Under the infinite twist condition we have the same result as for diffeomorphisms.

THEOREM 1.3. *An orientation reversing twist map of the plane that satisfies the infinite twist condition and that has a type I period-4 point, is a chaotic system — chaotic as explained in Theorem 1.2. Conversely, there exists an orientation reversing twist map that satisfies the infinite twist condition, has a type II period-4 point, and that has zero entropy.*

We can also give a lower bounds on the entropy for Theorems 1.2 and 1.3. Namely the entropy satisfies $h(f) \geq \frac{1}{2}\ln(1+\sqrt{2})$ and $h(f) \geq \frac{1}{2}\ln 3$ in Theorems 1.2 and 1.3 respectively.

The infinite twist condition makes the topological/variational principle we use easier to apply and the proof less technical. This is strongly related to the fact that the infinite twist condition is a more natural assumption in the context of twist maps than bijectivity. We will therefore explain all the details by proving Theorem 1.3. In Section 7 we make the necessary technical adaptations to the method in order to prove Theorem 1.2.

The method discussed in this paper makes extensive use of the twist property. On the other hand, we stress that it needs no compactness conditions, nor information about the asymptotics of f near infinity. It allows us to study periodic solutions of orientation reversing twist maps, in particular those of which the period is a multiple of four (but other periods can be dealt with as well). Theorems 1.2 and 1.3 are representative for the kind of results that can be obtained, but the method is much more general. We note that there is an additional variational structure that can be exploited in this setting if the (absolute value of the) area is preserved (see Remarks 2.2 and 3.8).

Of course the theorem does not detect all occurrences of chaos. An important example of orientation reversing twist maps is the Hénon map $f(x,y) = (\beta y, 1-\alpha y^2 + x)$, where $\alpha \in \mathbb{R}$ and $\beta > 0$ are parameters. It is well known that for various parameter choices the system is chaotic, while a type I period-4 point is hard/impossible to find. Nevertheless, concerning the practical aspects of the above theorem we note that to establish chaos one can search for

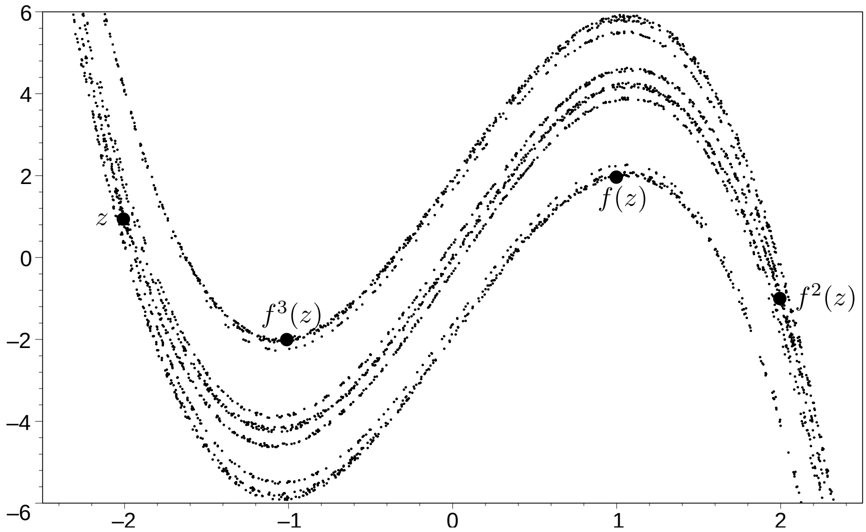

FIGURE 2. Orbits of the map $f(x,y) = (y, x + \frac{17}{3}y - \frac{5}{3}y^3)$. A period-4 orbit of type I is indicated by the large dots.

a type I period-4 point with the help of a computer. This can be done in a mathematically rigorous manner, for example with the help of a software package like GAIO, see [**14, 12**]. Furthermore, in the family of generalized Hénon maps $f(x,y) = (y, x + ay - by^3)$, which are orientation reversing twist maps, a period-4 orbit of type I can be found analytically (exploiting the symmetry) for $a > 4\sqrt{2}$ and any $b > 0$. In Figure 2 a period-4 orbit of type I is indicated and the chaotic nature of the dynamics is apparent.

To obtain an example of a non-chaotic map with a period-4 orbit of type II we return to the classical Hénon map, for convenience rescaled to read $f(x,y) = (y, \varepsilon x + \lambda[y - y^2])$. For $\varepsilon = 0$ this is a one dimensional map and for λ not too large it is non-chaotic. For small positive ε the 1-dimensional map perturbs to a 2-dimensional map, which for appropriately chosen λ has a period-4 point of type II and which remains non-chaotic. The details of the construction are given in Section 6. This provides a proof of second statements in Theorems 1.2 and 1.3.

We like to point out the similarity of the above theorem and the famous Sharkovskii theorem [**25, 19**], which states that a one dimensional system having a period-3 point necessarily has periodic points of all periods. In our case chaos is forced by certain period-4 points. In a one dimensional system the Sharkovskii ordering has little implications for a map containing a period-4 point. Nevertheless, also in the one dimensional case certain types of period-4 orbits (depending on the permutation of the points) force chaos (proved via the usual one dimensional techniques).

On compact surfaces of genus G (with or without boundary) the results in [**16**] and [**6**] show that if an orientation reversing diffeomorphism has at least $G+2$ periodic points of distinct odd periods, then there exist periodic points for infinitely many different periods, and in particular the topological entropy of the map is positive. The maps in this paper are maps on $\mathbb{R}^2$ and therefore the above result does not immediately apply. However, in the special circumstance that an orientation reversing map on $\mathbb{R}^2$ allows extension to S^2 with a fixed point at infinity, then the existence of a period-3 point, or any other odd period for that matter, implies, by the above mentioned result, that the map has positive topological entropy. To translate this result back to the context of the original map on $\mathbb{R}^2$ one needs (detailed) information about the local behavior near the point at infinity (the asymptotics of the map). In contrast, Theorems 1.2 and 1.3 are applicable without prior knowledge of asymptotic behavior. Moreover, our result gives insight in what happens when we have information about period-4 points, which complements the results on periodic orbits with odd periods in [**6, 16**].

The relation to Thurston's theory. Once again, the method of proof in this paper strongly relies on the fact that we consider (compositions of) twist maps, which allows an elementary construction of infinitely many periodic points and a semi-conjugacy to a (sub-)shift on 3 symbols. This draws strongly on the elegant topological principle for twist maps. A different approach would be to employ Thurston's classification theorem of surface diffeomorphisms [**26**]. Thurston's result does not restrict to twist maps, however compactness is required (we come back to this point in a moment).

Since the results for arbitrary maps on compact surfaces via Thurston's theory are complementary to those for twist maps on the (non-compact) plane in the present paper, let us explain how our results relate to Thurston's theory. For sake of simplicity, let us assume that the maps can be extended to homeomorphisms on for example D^2. In that case the classification theorem is applicable. In order to follow the approach using Thurston's classification theorem we first need to decide what distinguishes period-4 points. In our approach there is a natural distinction into two types of period-4 points via discrete four strand braids. In

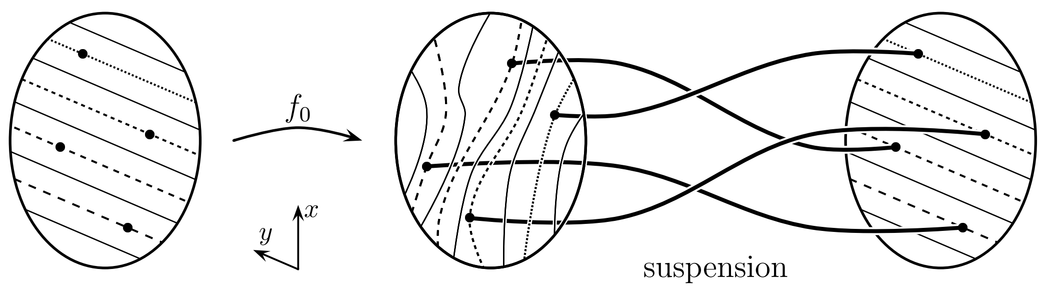

FIGURE 3. The map f_0 is orientation preserving and has the twist property, hence the suspension looks like a distorted rotation, which leads to a positive braid.

the approach using Thurston's result the braids are used to determine the isotopy class of a map in question, see e.g. [**8**].

It is easier to visualize this for orientation preserving maps, so we consider $g = f^4$, which is an orientation preserving map and which can be written as a composition of four orientation preserving positive twist maps $g = f_3 \circ f_2 \circ f_1 \circ f_0$. In the case of a period-4 orbit $P = \{f^i(z)\}_{i=0}^3$ for f, the map g has four fixed points P. Therefore one considers the mapping class group $\mathrm{MCG}(D^2 \text{ rel } P)$, where the maps are orientation preserving and fix P (as a set) and ∂D^2 (a homeomorphism of the boundary). Using the results in [**5**] it can be shown easily that $\mathrm{MCG}(D^2 \text{ rel } P) \simeq B_4/\text{center}$, where B_4 is Artin's braid group on four strands, and the center of the braid group B_4 is the infinite cyclic subgroup generated by $(\sigma_1\sigma_2\sigma_3)^4$, the full twists.

In general it is quite hard to determine the mapping class of a map, but for twist maps this is a little easier. In fact, identifying the mapping class with the braid group, the mapping class for f^4 is exactly the positive braid we have constructed above. We illustrate this for the first of the composite maps f_0 for a type I period-4 orbit in Figure 3. Besides the permutation of the (x-coordinates of the) points in P, the twist property gives global information about the map, so that the suspension can be understood (note that f_0 does not fix P, but this does not lead to undue complications). The other three maps are similar and the total braid is obtained by the natural addition in the braid group. We refer to [**7**] for a further discussion on the application of Thurston's theory to twist maps on an annulus. As a final point, the same construction can be carried out for $\tilde{g} = f^2 = f_+ \circ f_-$. One needs to take into account that f_- has negative twist and thus leads to a braid with negative generators. Of course, repeating the braid for $\tilde{g}$ twice leads to a braid that is equivalent to the one for g.

Using Thurston's classification the braid of type I is pseudo-Anosov, and thus the corresponding mapping class is also pseudo-Anosov, hence chaotic. In order to draw conclusions for the original map on $\mathbb{R}^2$ one needs to find a compact invariant set in the *interior* of D^2 on which the entropy is positive. This requires detailed information about the behavior near ∂D^2, and thus about the asymptotic behavior of the original map on $\mathbb{R}^2$. This is *not* needed in our results however. The braid of type II is reducible and contains only components of finite type (and thus no pseudo-Anosov component, in fact the braid is a cable of cabled braids), hence the corresponding map is not necessarily chaotic. We point out that our construction of a non-chaotic map with a type II period-4 point confirms the latter conclusion. However, Thurston's classification theorem does not provide a non-chaotic map within the class of twist maps as required here. See also [**9**] for details on pseudo-Anosov maps and mapping classes.

The organization of the paper is as follows. In Section 2 we recall some facts about twist maps and for orientation reversing maps we introduce a transformation that associates a parabolic recurrence relation to such maps. In Section 3 we summarize the concepts we need from braid theory and parabolic flows, which were thoroughly studied in [**15**]. In Section 4 the focus shifts to period-4 orbits and their classification in types I and II. We combine these concepts in Section 5 to prove the first assertion in Theorem 1.3 by constructing a semi-conjugacy to the shift on three symbols. In Section 6 we show an example of a non-chaotic map with a period-4 orbit of type II, which establishes the second part of the theorem. Finally, Section 7 is devoted to extending the techniques to bijective maps and proving Theorem 1.2.

Acknowledgement. The authors wish to thank R.W. Ghrist for a number of fruitful discussions on this subject.

2. Twist Maps

We collect some facts about both orientation preserving and reversing twist maps.

2.1. Recurrence relations for twist maps. A C^1 map from $\mathbb{R}^2$ to $\mathbb{R}^2$, denoted by $f(x,y) = (\pi_x f, \pi_y f)$, is a (positive) twist map if $\frac{\partial \pi_x f}{\partial y} > 0$. It is orientation preserving if

$\det(df) > 0$ and orientation reversing if $\det(df) < 0$. Of course, one could also consider $\frac{\partial \pi_y f}{\partial x} > 0$ and/or negative twist, but a change of coordinates reduces these cases to $\frac{\partial \pi_x f}{\partial y} > 0$.

Note that iterates f^k of a twist map are not necessarily twist maps, but the crucial property of twist maps is that they allow us to retrieve whole trajectories $\{(x_k, y_k)\} = \{f^k(x_0, y_0)\}$ from just the sequence $\{x_k\}$. To show this we follow [**2**] (see also [**1**]). Let us start with the observation that the twist property implies that there exists an open set U such that for any pair $x, x' \in U$ there exists a unique solution $Y(x, x')$ of the equation

$$\pi_x f(x, Y(x, x')) = x'.$$

It also follows from the twist property that Y is monotone in x':

$$\frac{\partial Y}{\partial x'} > 0.$$

From the function Y we construct yet another function:

$$\widetilde{Y}(x, x') \stackrel{\text{def}}{=} \pi_y f(x, Y(x, x')).$$

This second function $\widetilde{Y}$ also has a monotonicity property that follows directly from the inverse function theorem. The map f is locally invertible and the derivative of its inverse f^{-1} is given by $\partial_2(\pi_x f^{-1}) = -(\det(df))^{-1}\partial_2(\pi_x f) \circ f^{-1}$, hence

$$\begin{aligned} &\partial_2(\pi_x f^{-1}) < 0 \quad \text{and} \quad \frac{\partial \widetilde{Y}}{\partial x} < 0 \qquad \text{if } f \text{ is orientation preserving,} \\ &\partial_2(\pi_x f^{-1}) > 0 \quad \text{and} \quad \frac{\partial \widetilde{Y}}{\partial x} > 0 \qquad \text{if } f \text{ is orientation reversing.} \end{aligned}$$

Obviously the reason for these definitions is that if $(x_{k+1}, y_{k+1}) = f(x_k, y_k)$ then

$$y_k = Y(x_k, x_{k+1}) \qquad \text{and} \qquad y_{k+1} = \widetilde{Y}(x_k, x_{k+1}).$$

That is, the functions Y and $\widetilde{Y}$ can be used to retrieve the whole trajectory $\{(x_k, y_k)\}$ from the sequence $\{x_k\}$. It easily follows that a sequence $\{(x_k, y_k)\}$ forms an orbit of f if and only if the x-coordinates satisfy

$$Y(x_k, x_{k+1}) - \widetilde{Y}(x_{k-1}, x_k) = 0 \qquad \text{for all } k \in \mathbb{Z}.$$

We therefore introduce the notation

$$\mathcal{R}(x_{k-1}, x_k, x_{k+1}) \stackrel{\text{def}}{=} Y(x_k, x_{k+1}) - \widetilde{Y}(x_{k-1}, x_k). \tag{3}$$

Solutions $\{x_k\}$ of the recurrence relation $\mathcal{R}(x_{k-1}, x_k, x_{k+1}) = 0$ thus correspond to trajectories of the map f. From the properties of Y and $\widetilde{Y}$ we see that $\mathcal{R}$ is increasing in x_{k+1}, and if f is orientation preserving then $\mathcal{R}$ is also increasing in x_{k-1}. In this case $\mathcal{R}$ will be referred to as a *parabolic recurrence relation*. When f is orientation reversing then $\mathcal{R}$ is not increasing, but decreasing in x_{k-1}. In Section 2.2 we explain how we can, nevertheless, associate a parabolic recurrence relation to an orientation reversing map.

The function Y (and similarly $\widetilde{Y}$) has a domain of the form

$$D = \{(x, x') \,|\, x \in \mathbb{R}, g(x) < x' < h(x)\},$$

where the functions $g, h : \mathbb{R} \to [-\infty, \infty]$ are upper/lower semi-continuous with $g(x) < h(x)$, see Section 7 for more details. A way to ensure that the domain D is the whole plane, is to assume the *infinite twist* condition (2). To simplify the exposition in the following sections we assume that $D = \mathbb{R}^2$. In Section 7 we show how to extend our results to maps that are bijective to $\mathbb{R}^2$ (i.e. diffeomorphisms of the plane). Note that bijectivity does not imply the infinite twist condition, nor does it guarantee that $D = \mathbb{R}^2$.

Remark 2.1. Any twist map that satisfies the infinite twist condition is injective. Namely, let $f(x_0, y_0) = f(x_1, y_1) = (x', y')$. If $x_0 = x_1$ then it follows from the twist property that $y_0 = y_1$. Suppose $x_0 \neq x_1$, say $x_0 < x_1$, then the infinite twist condition implies that for any $x \in [x_0, x_1]$ there is a (unique) $y(x)$ such that $\pi_x f(x, y(x)) = x'$, with $y(x_0) = y_0$ and $y(x_1) = y_1$. Since $\frac{\partial \widetilde{Y}(x,x')}{\partial x} \lesseqgtr 0$ we have $\frac{d\pi_y f(x,y(x))}{dx} \lesseqgtr 0$, contradiction the fact that $\pi_y f(x_0, y(x_0)) = \pi_y f(x_1, y(x_1)) = y'$.

Remark 2.2. When f is an orientation and *area* preserving twist map there exists an additional structure, namely generating functions (see e.g. [**3**]). A smooth function $S : \mathbb{R}^2 \to \mathbb{R}$ exists with the property that if $(x', y') = f(x, y)$, then $y = \partial_1 S(x, x')$, and $y' = -\partial_2 S(x, x')$. This generating function S allows one to formulate the existence of periodic points in terms of critical points of an action function. A period-n point corresponds to a critical point of

$$W(x_0, x_1, \ldots, x_{n-1}) \stackrel{\text{def}}{=} \sum_{i=0}^{n-1} S(x_i, x_{i+1}), \qquad \text{with } x_n = x_0.$$

The parabolic recurrence relation is then given by the gradient of W: $\mathcal{R}(x_{i-1}, x_i, x_{i+1}) = \frac{\partial W}{\partial x_i}$. For orientation reversing area preserving maps a similar variational structure exists. The difference is that the relations between the generating function S and the y coordinates are

$y = \partial_1 S(x, x')$ and $y' = \partial_2 S(x, x')$, i.e. with the same sign. A period-$2m$ point corresponds to a critical point of

$$W(x_0, x_1, \ldots, x_{2m-1}) \stackrel{\text{def}}{=} \sum_{i=0}^{2m-1} (-1)^i S(x_i, x_{i+1}), \qquad \text{with } x_{2m} = x_0.$$

The recurrence relation is not quite given by the gradient, but by $\frac{\partial W}{\partial x_i} = (-1)^i \mathcal{R}(x_{i-1}, x_i, x_{i+1})$, so there is still a correspondence between critical points of W and solutions of $\mathcal{R}$. However, it is more convenient to deal with such a situation through the (flip) transformation described in Section 2.2 below.

We finish this section with an example.

Example 2.3. Let us consider the well known *Hénon map*. The Hénon map is a two-dimensional invertible map given by formula:

$$f : \begin{pmatrix} x \\ y \end{pmatrix} \mapsto \begin{pmatrix} \beta y \\ 1 - \alpha y^2 + x \end{pmatrix}.$$

It is an orientation reversing twist map for all $\beta > 0$ and $\alpha \in \mathbb{R}$. It is bijective and also satisfies the infinite twist condition (2). It is not difficult to construct the recurrence relation:

$$\mathcal{R}(x_{k-1}, x_k, x_{k+1}) = -1 - x_{k-1} + \alpha\beta^{-2} x_k^2 + \beta^{-1} x_{k+1}.$$

2.2. Parabolic recurrence relations for orientation reversing twist maps. Consider the case that f is an orientation *reversing* twist map. From the previous subsection it then follows that the trajectory of a periodic point can be retrieved from the sequence $\{x_k\}$ satisfying the recurrence relation

$$\widetilde{\mathcal{R}}(x_{k-1}, x_k, x_{k+1}) = 0,$$

where $\widetilde{\mathcal{R}}$ is defined by (3), with $\partial_1 \widetilde{\mathcal{R}} < 0$ and $\partial_3 \widetilde{\mathcal{R}} > 0$. Since the theory of braid flows (see Section 3.2) is defined using parabolic recurrence relations (i.e. $\partial_1 \mathcal{R} > 0$ and $\partial_3 \mathcal{R} > 0$), we need to make a modification. In Section 1 we explained that f^4 can be written as a composition of four orientation preserving positive twist maps f_i. For each f_i we can derive the recurrence function $\mathcal{R}_i$, which has the properties that

$$\partial_1 \mathcal{R}_i > 0 \qquad \text{and} \qquad \partial_3 \mathcal{R}_i > 0.$$

This is equivalent to defining the functions $\mathcal{R}_i$ as follows

$$\begin{aligned}
\mathcal{R}_0(x_{-1}, x_0, x_1) &\stackrel{\text{def}}{=} \widetilde{\mathcal{R}}(-x_{-1}, -x_0, x_1) \\
\mathcal{R}_1(x_0, x_1, x_2) &\stackrel{\text{def}}{=} \widetilde{\mathcal{R}}(-x_0, x_1, x_2) \\
\mathcal{R}_2(x_1, x_2, x_3) &\stackrel{\text{def}}{=} -\widetilde{\mathcal{R}}(x_1, x_2, -x_3) \\
\mathcal{R}_3(x_2, x_3, x_4) &\stackrel{\text{def}}{=} -\widetilde{\mathcal{R}}(x_2, -x_3, -x_4).
\end{aligned}$$

It is easily verified that the recurrence functions are indeed parabolic and we define the sequence $\{\mathcal{R}_i\}$ periodically: $\mathcal{R}_{i+4} = \mathcal{R}_i$. This change of coordinates naturally also effects the trajectory $x = \{x_k\}$. To make this precise we define the transformation

$$\lambda(x)_k = \begin{cases} -x_k & \text{for } k = 0, 3 \bmod 4 \\ x_k & \text{for } k = 1, 2 \bmod 4 \end{cases} \tag{4}$$

We call the transformation λ on sequences a *flip*. Clearly $\lambda^2 = \text{id}$ and it commutes with σ^4, where σ is the shift map $\sigma(x)_k = x_{k+1}$. Now $x = \{x_k\}$ solves $\widetilde{\mathcal{R}} = 0$ if and only if $\lambda(x)$ solves $\mathcal{R}_i = 0$.

LEMMA 2.4. *Every solution $x = \{x_k\}$ of $\mathcal{R}_i = 0$ yields a solution $\lambda(x)$ of $\widetilde{\mathcal{R}} = 0$, and thus corresponds to a trajectory of f, namely $\big\{\big(\lambda(x)_k, Y(\lambda(x)_k, \lambda(x)_{k+1})\big)\big\}$.*

3. Braid diagrams and the Conley index

3.1. Discretized braids and braid diagrams. In this section we define and describe the main topological structure which is used in the proofs of Theorems 1.2 and 1.3. As pointed out in Section 1 the way we deal with sequences is to consider them as piecewise linear functions by connecting the consecutive points via linear interpolation.

DEFINITION 3.1 ([**15**]). The space of *discretized period d braids on n strands,* denoted $\mathcal{D}^n_d$, is the space of all pairs $(\mathbf{u}, \tau)$, where $\tau \in S_n$ is a permutation on n elements, and $\mathbf{u}$ is an unordered collection of n strands $\mathbf{u} = \{\mathbf{u}^\alpha\}_{\alpha=1}^n$, which satisfy the following properties:

(a) Each strand consist of $d+1$ anchor points: $\mathbf{u}^\alpha = (u_0^\alpha, u_1^\alpha, \dots, u_d^\alpha) \in \mathbb{R}^{d+1}$.

(b) *periodicity* – For all $\alpha = 1, \dots, n$, one has: $u_d^\alpha = u_0^{\tau(\alpha)}$.

(c) *transversality* – For any pair of distinct strands α and α' such that $u_i^\alpha = u_i^{\alpha'}$ for some i, we have:

$$(u_{i-1}^\alpha - u_{i-1}^{\alpha'})(u_{i+1}^\alpha - u_{i+1}^{\alpha'}) < 0. \tag{5}$$

We equip $\mathcal{D}_d^n$ with the standard topology of $\mathbb{R}^{nd}$ on the strands, and the discrete topology with respect to the permutation τ, modulo permutations which change the order of the strands (i.e., two pairs $(\mathbf{u},\tau)$ and $(\tilde{\mathbf{u}},\tilde{\tau})$ are close if there exists a permutation $\sigma\in S_n$ with $\sigma\circ\tilde{\tau}=\tau\circ\sigma$), such that $\mathbf{u}^{\sigma(\alpha)}$ is close to $\tilde{\mathbf{u}}^{\alpha}$ (as points in $\mathbb{R}^{nd}$) for all α.

We will say that two discretized braids $\mathbf{u},\mathbf{u}'\in\mathcal{D}_d^n$ are of the same *discretized braid class* (denoted $[\mathbf{u}]=[\mathbf{u}']$) if they are in the same path component of $\mathcal{D}_d^n$. The discrete topology on the permutations leads to the following useful interpretation. Consider a continuous family of braids and pick one of the permutations in the equivalence class (subsequently dropped from the notation). These discretized braids of period d on n strands are then completely determined by their coordinates $\{u_i^\alpha\}_{i=1\dots d}^{\alpha=1\dots n}$, i.e., every discretized braid corresponds to a point in the configuration space $\mathbb{R}^{nd}$. We come back to this point of view later.

Let us now compare the notion of a discretized braid with that of a topological braid. In topology a braid β on n strands is a collection of embeddings $\{\beta^\alpha:\,[0,1]\to\mathbb{R}^3\}_{\alpha=1}^n$ with disjoint images such that (a) $\beta^\alpha(0)=(0,\alpha,0)$, (b) $\beta^\alpha(1)=(1,\tau(\alpha),0)$ for some permutation $\tau\in S_n$, and (c) the image of each β^α is transverse to all the planes $\{x=\text{constant}\}$.

The projection of a topological braid onto an appropriate plane, e.g. the (x,y)-plane, is called a *braid diagram* if all crossings of strands are transversal in this projection. In this braid diagram a marking $(+)$ indicates a crossing which is "bottom over top", whereas a marking $(-)$ indicates a crossing "top over bottom". A positive $(+)$ crossing of the i-th and $(i+1)$-st strands corresponds to a generator σ_i, while a negative crossing corresponds to σ_i^{-1}. The use of these generators σ_i leads to a natural group structure (see e.g. [**5**] for more background). The sequence of generators ("reading" the braid from left to right) is called the braid word.

The link between discretized braids and topological braids is the following. Any discretized braid $\mathbf{u}$ can be interpreted as the braid diagram of a topological braid when we use linear interpolation between the points $(i,u_i^\alpha)\in\mathbb{R}^2$, where u_i^α are the anchor points of strand α. Here we choose the convention that all crossings in this discretized braid diagram are *positive*. The resulting positive piecewise linear braid diagram is denoted by $\beta(\mathbf{u})$. It is also useful to consider braid diagrams that are not piecewise linear. A (positive, closed) topological braid diagram is a collection of strands $\{\beta^\alpha\in C([0,1])\}_{\alpha=1}^n$ such that (a) $\beta^\alpha(1)=\beta^{\tau(\alpha)}(0)$ for some permutation $\tau\in S_n$, and (b) all intersections among pairs of strands are isolated

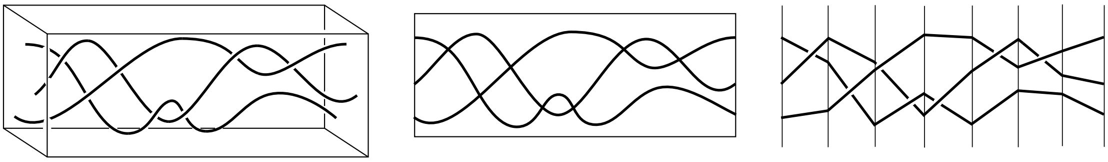

FIGURE 4. Example of a braid on three strands. [left] A braid with all crossings positive (bottom over top), [middle] its 2-d projection, and [right] the associated piecewise linear braid diagram, a discretized braid. Its braid word is $\sigma_2\sigma_1\sigma_2\sigma_1^2\sigma_2^2$.

and topologically transverse. The *topological braid class* $\{\mathbf{u}\}$ is a path component of $\beta(\mathbf{u})$ in the space of positive topological braid diagrams. Figure 4 depicts a braid in its various appearances. Since for positive braids the braid word consists of positive generators only, it follows that the number of generators in the braid word, the *braid word length*, is an invariant of a discretized braid class, and even of a topological braid class. For a more detailed account we refer to [**15**].

Since discretized braids are periodic we extend all strands periodically:

$$u_{i+d}^{\alpha} = u_i^{\tau(\alpha)} \qquad \text{for all } i \in \mathbb{Z}, \quad \alpha = 1, \ldots, n.$$

As explained above, $\mathcal{D}_d^n$ is a subset of a collection of copies of $\mathbb{R}^{nd}$ (one for each equivalence class of permutations). Fixing an appropriate permutation, we may identify a discretized braid class with a subset of $\mathbb{R}^{nd}$, its configuration space. The connected components of $\mathcal{D}_d^n$, i.e. the discretized braid classes, are separated by co-dimension-1 varieties in $\mathbb{R}^{nd}$, called the singular braids:

DEFINITION 3.2. Let $\overline{\mathcal{D}}_d^n$ denote the collection of nd-dimensional vector spaces of all discretized braid diagrams $\mathbf{u}$ satisfying properties (1) and (2) of Definition 3.1. Now $\Sigma \stackrel{\text{def}}{=} \overline{\mathcal{D}}_d^n \setminus \mathcal{D}_d^n$ is the set of *singular discretized braids.*

The set $\overline{\mathcal{D}}_d^n$ is the closure of $\mathcal{D}_d^n$, hence its elements do not necessarily satisfy the transversality condition (5). The braids in Σ are said to have a *tangency.* A moments reflection shows that in singular braids of sufficiently high co-dimension ($m \geq d$), different strands can collapse onto each other. This set of specific singularities plays an important role later on and is defined as

$$\Sigma^- \stackrel{\text{def}}{=} \{\mathbf{u} \in \Sigma \,|\, u_i^{\alpha} = u_i^{\alpha'}, \forall i \in \mathbb{Z}, \text{ for some } \alpha \neq \alpha'\}.$$

If one wants to braid a strand, one needs something to braid it through. This leads us to the introduction of a so-called *skeleton* braid through which we can braid so-called *free* strands. Define $\mathbf{u}\cup\mathbf{v} \in \overline{\mathcal{D}}_d^{n+m}$, with $\mathbf{u} \in \overline{\mathcal{D}}_d^n$ and $\mathbf{v} \in \overline{\mathcal{D}}_d^m$ as the (unordered) union of strands. Then for given a $\mathbf{v} \in \mathcal{D}_d^m$ we define

$$\mathcal{D}_d^n \text{ REL } \mathbf{v} \stackrel{\text{def}}{=} \{\mathbf{u} \in \mathcal{D}_d^n \,|\, \mathbf{u} \cup \mathbf{v} \in \mathcal{D}_d^{n+m}\}.$$

It is important to remember that the transversality condition (5) is imposed on the strands in $\mathbf{u} \cup \mathbf{v}$.

The path components of $\mathcal{D}_d^n$ REL $\mathbf{v}$ form *relative discretized braid classes*, denoted by $[\mathbf{u} \text{ REL } \mathbf{v}]$. The braid $\mathbf{v}$ is usually called the *skeleton*, and $\mathbf{u}$ are called the *free strands.* Now it is easy to define relative versions of the concepts presented above, i.e. Σ REL $\mathbf{v}$, Σ^- REL $\mathbf{v}$, $\overline{\mathcal{D}}_d^n$ REL $\mathbf{v}$, and $\{\mathbf{u} \text{ REL } \mathbf{v}\}$ (as *topological relative braid class*).

It is also possible that two classes $[\mathbf{u} \text{ REL } \mathbf{v}]$ and $[\mathbf{u}' \text{ REL } \mathbf{v}']$ are topologically the same. The set of equivalent topological relative braid classes $\big\{\mathbf{u} \text{ REL } \{\mathbf{v}\}\big\}$ is defined by the relation $\{\mathbf{u} \text{ REL } \mathbf{v}\} \sim \{\mathbf{u}' \text{ REL } \mathbf{v}'\}$ if and only if there exist a continuous family of topological (positive, closed) braid diagram pairs deforming $(\mathbf{u}, \mathbf{v})$ to $(\mathbf{u}', \mathbf{v}')$. See [**15**] for more details.

3.2. Parabolic flows on braid diagrams. In [**15**] the topology of discretized braids is used to find solutions of parabolic recurrence relations. This is done by embedding the problem into an appropriate dynamical setting. Before briefly explaining the ideas we recall the definition of parabolic recurrence relations.

Definition 3.3 ([**15**]). A sequence of functions $\mathcal{R} = (\mathcal{R}_i)_{i\in\mathbb{Z}}$, with $\mathcal{R}_i \in C^1(\mathbb{R}^3, \mathbb{R})$, satisfying

(i) $\partial_1\mathcal{R}_i > 0$ and $\partial_3\mathcal{R}_i \geq 0$ for all $i \in \mathbb{Z}$,
(ii) for some $d \in \mathbb{N}$ we have $\mathcal{R}_{i+d} = \mathcal{R}_i$ for all $i \in \mathbb{Z}$,

is called a *parabolic recurrence relation.*

Here we only consider parabolic recurrence relations defined on $\mathbb{R}^3$, although one can also study parabolic recurrence relations on more general domains, see Section 7.

Let $\mathcal{R}$ be a parabolic recurrence relation and consider the differential equation

$$\frac{du_i}{dt} = \mathcal{R}_i(u_{i-1}, u_i, u_{i+1}) \quad \text{where } \mathbf{u}(t) \in \mathbf{X} = \mathbb{R}^{\mathbb{Z}} \text{ and } t \in \mathbb{R}.$$

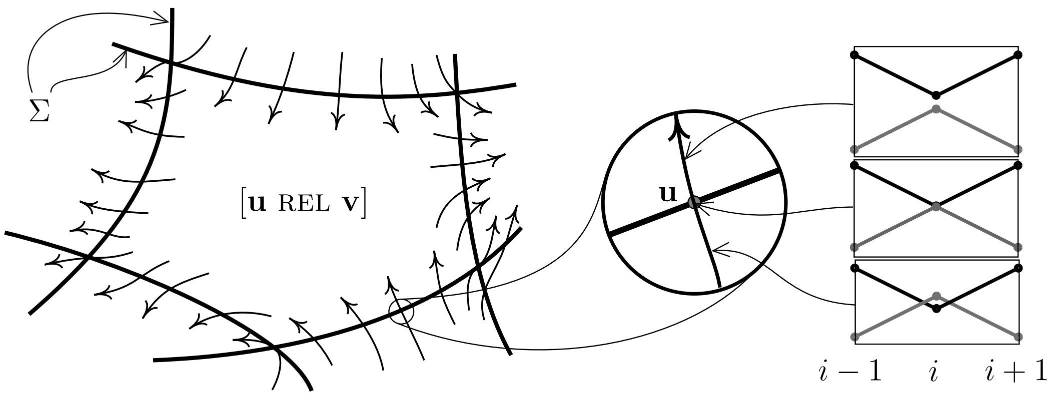

FIGURE 5. A schematic picture of a parabolic flow on a (bounded and proper) braid class.

It is straightforward to show that such an equation defines a (local) C^1-flow ψ^t on $\mathbf{X}$ under periodic boundary conditions, provided they are of period nd. We call such a flow, generated by a parabolic recurrence relation, a *parabolic flow* on $\mathbf{X}$. Notice that it is easy to regard this flow as a flow on the space $\overline{\mathcal{D}}^n_d$ by considering the equation

$$\frac{du_i^\alpha}{dt} = \mathcal{R}_i(u_{i-1}^\alpha, u_i^\alpha, u_{i+1}^\alpha), \quad \text{where } \mathbf{u} \in \overline{\mathcal{D}}^n_d. \tag{6}$$

This equation is well-defined by the periodicity requirement in Definition 3.3. The next-neighbor coupling and the monotonicity of a parabolic recurrence relation have far reaching consequences for the corresponding parabolic flow. Namely, along flow lines the total number of intersections in a braid, i.e. the braid word length, can only decrease in time (as indicated in Figure 5). The following proposition is a precise statement of this property.

PROPOSITION 3.4 ([**15**]). *Let ψ^t be a parabolic flow on $\overline{\mathcal{D}}^n_d$.*

(a) *For each point $\mathbf{u} \in \Sigma \setminus \Sigma^-$, the local orbit $\{\psi^t(\mathbf{u}) \mid t \in [-\varepsilon, \varepsilon]\}$ intersects Σ uniquely at $\mathbf{u}$ for all ε sufficiently small.*

(b) *For any such $\mathbf{u}$, the braid word length of the braid diagram $\psi^t(\mathbf{u})$ for $t > 0$ is strictly less then that of the braid diagram $\psi^t(\mathbf{u})$ for $t < 0$.*

As a direct consequence of this proposition flow lines cannot re-enter a braid class after leaving it. In other words, the dynamics of (6) obeys the natural co-orientation of the braid classes, i.e., if we co-orient the boundary $\Sigma \setminus \Sigma^-$ in the direction of decreasing intersection number, then the vector field, and thus the flow, is co-oriented in the same way.

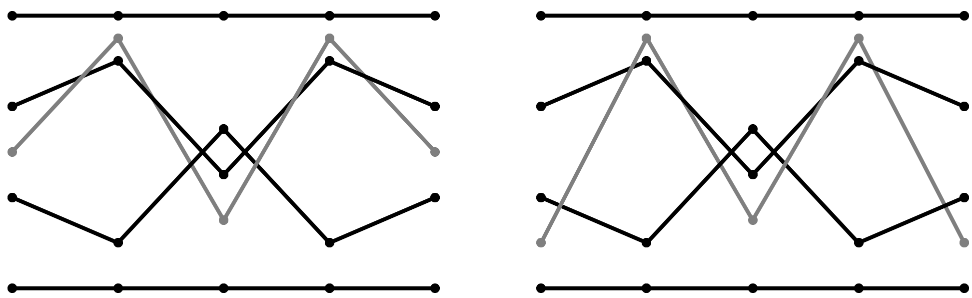

FIGURE 6. Two bounded braids with the same skeleton (black lines); the free strand is the gray line. The braid on the left is improper (one can deform the free strand to one of the strands of the skeleton), the one on the right is proper.

In Section 3.3 we will define the Conley index of a braid class, hence we need the braid class to be isolating, i.e., the flow at the boundary should have no internal tangencies. Proposition 3.4 shows that we are "in danger" when our system evolves near to Σ^-, since a parabolic flow displays invariant behavior in Σ^-. For this reason, a discretized relative braid class $[\mathbf{u} \text{ REL } \mathbf{v}]$ is called *proper* if its boundary (which is a subset of $\Sigma \text{ REL } \mathbf{v}$) does not intersect $\Sigma^- \text{ REL } \mathbf{v}$. Figure 6 gives a simple examples of a proper and an improper braid class. Besides properness we also need the braid classes to be compact. A discretized relative braid class $[\mathbf{u} \text{ REL } \mathbf{v}]$ is called *bounded* if the set $[\mathbf{u} \text{ REL } \mathbf{v}] \subset \mathbb{R}^{(n+m)d}$ is bounded.

3.3. Conley index for braids. The Conley index is a powerful tool for studying the complexity of dynamical systems. For braid classes the Conley index is defined in [**15**] and we refer to that paper for all details, proofs and much additional information. For more details about the general setting of the Conley index, see [**11, 21**]. Proposition 3.4 implies that $\mathrm{cl}([\mathbf{u} \text{ REL } \mathbf{v}])$ is isolating for the flow generated by a parabolic recurrence relation, provided the braid class is proper and bounded. Let N denote $\mathrm{cl}([\mathbf{u} \text{ REL } \mathbf{v}])$, and let $N^- \subset \partial N$ be the exit set for a parabolic flow ψ^t. Then the Conley index $h(\mathbf{u} \text{ REL } \mathbf{v})$ is the homotopy type of the pointed space $(N/N^-, [N^-])$, denoted by $[N/N_-]$. Note that N^- can also be characterized purely in terms of braids by using the co-orientation of $\Sigma \setminus \Sigma^-$.

PROPOSITION 3.5 ([**15**]). *Suppose* $[\mathbf{u} \text{ REL } \mathbf{v}]$ *is a bounded proper relative discretized braid class and* ψ^t *is a parabolic flow that fixes the skeleton* $\mathbf{v}$*. Then*

(1) $\mathrm{cl}([\mathbf{u}\ \mathrm{REL}\ \mathbf{v}])$ *is an isolating neighborhood for* ψ^t, *which yields a well-defined Conley index* $h(\mathbf{u}\ \mathrm{REL}\ \mathbf{v}, \psi^t)$.

(2) *The index* $h(\mathbf{u}\ \mathrm{REL}\ \mathbf{v}, \psi^t)$ *is independent of the choice of the parabolic flow* ψ^t *as long as* $\psi^t(\mathbf{v}) = \mathbf{v}$. *Therefore the index is denoted by* $h(\mathbf{u}\ \mathrm{REL}\ \mathbf{v})$.

Remark 3.6. The Conley index is in fact an invariant of the topological relative braid class $\{\mathbf{u}\ \mathrm{REL}\ \mathbf{v}\}$, provided one slightly generalizes the definitions. First, the definitions of proper and bounded are extended in a straightforward manner to $\{\mathbf{u}\ \mathrm{REL}\ \mathbf{v}\}$. Furthermore, an equivalence class of topological relative braids $\{\mathbf{u}\ \mathrm{REL}\ \{\mathbf{v}\}\}$ is proper/bounded if for all $\mathbf{v}' \in \{\mathbf{v}\}$ any class $\{\mathbf{u}'\ \mathrm{REL}\ \mathbf{v}'\} \in \{\mathbf{u}\ \mathrm{REL}\ \{\mathbf{v}\}\}$ is proper/bounded.

Second, several discretized braid classes may be part of equivalent topological braid classes. For fixed period d, let $[\mathbf{u}(0)\ \mathrm{REL}\ \mathbf{v}']$ be a discretized braid class such that on the topological level $\{\mathbf{u}(0)\ \mathrm{REL}\ \mathbf{v}'\} \in \big\{\mathbf{u}\ \mathrm{REL}\ \{\mathbf{v}\}\big\}$. Let $[\mathbf{u}(j)\ \mathrm{REL}\ \mathbf{v}']$, $j = 0, \ldots, m$ denote *all* the different discretized braid classes relative to $\mathbf{v}'$ such that $\{\mathbf{u}(j)\ \mathrm{REL}\ \mathbf{v}'\} \in \big\{\mathbf{u}\ \mathrm{REL}\ \{\mathbf{v}\}\big\}$. The set $\widetilde{N} = \bigcup_{j=0}^{m} \mathrm{cl}([\mathbf{u}(j)\ \mathrm{REL}\ \mathbf{v}'])$ is isolating for any parabolic flow fixing $\mathbf{v}'$, and the exit set is denoted by $\widetilde{N}^-$. The Conley index $\mathbf{H}(\mathbf{u}\ \mathrm{REL}\ \mathbf{v}')$ of the topological relative braid class $\{\mathbf{u}\ \mathrm{REL}\ \mathbf{v}'\}$ is the homotopy type of the pointed space $(\widetilde{N}/\widetilde{N}^-, [\widetilde{N}^-])$. It does not depend on the period d, the choice of $\mathbf{v}'$ or the parabolic flow. The Conley index $\mathbf{H}(\mathbf{u}\ \mathrm{REL}\ \mathbf{v}')$ is an invariant of $\big\{\mathbf{u}\ \mathrm{REL}\ \{\mathbf{v}\}\big\}$.

The homotopy index is usually not very convenient to work with and therefore we use the *homological* Conley index

$$CH_*(\mathbf{u}\ \mathrm{REL}\ \mathbf{v}) \stackrel{\mathrm{def}}{=} H_*(N, N^-)$$

where $N = \mathrm{cl}([\mathbf{u}\ \mathrm{REL}\ \mathbf{v}])$, N^- is its exit set, and H_* is the relative homology of the pair (N, N^-). One can assign to such an index a characteristic polynomial

$$CP_t(\mathbf{u}\ \mathrm{REL}\ \mathbf{v}) \stackrel{\mathrm{def}}{=} \sum_{k \geq 0} \beta_k t^k,$$

where β_k is a free rank of $CH_k(\mathbf{u}\ \mathrm{REL}\ \mathbf{v})$. For the parabolic flows under consideration Morse inequality can be used to draw conclusions from the characteristic polynomial about fixed points and periodic orbits (see Section 7 of [**15**]). In this paper we use the only the simplest consequence:

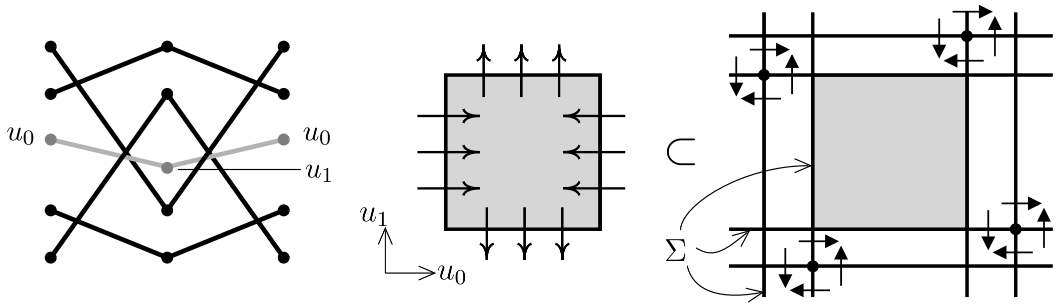

FIGURE 7. In the relative braid on the left black lines denote the skeleton and gray lines the free strand. In the middle its configuration space is shown and the direction of the parabolic flow on the boundary is indicated. On the right we see how the configuration space is positioned with respect to the stationary points of the skeleton, represented by the four dots.

LEMMA 3.7. *Let* $[\mathbf{u} \text{ REL } \mathbf{v}]$ *be a discretized relative braid class that is bounded and proper. If* $CP_{-1}(\mathbf{u} \text{ REL } \mathbf{v})$ *is nonzero, then there is at least one stationary point in* $[\mathbf{u} \text{ REL } \mathbf{v}]$ *for any parabolic flow* ψ^t *that leaves* $\mathbf{v}$ *invariant.*

REMARK 3.8. A special situation occurs when the recurrence relation is exact, i.e., when there exists a d-periodic sequence of $C^2(\mathbb{R}^2)$ functions S_i such that

$$\mathcal{R}_i(u_{i-1}, u_i, u_{i+1}) = \partial_2 S_{i-1}(u_{i-1}, u_i) + \partial_1 S_i(u_i, u_{i+1}) \qquad \text{for all } i \in \mathbb{Z}.$$

Note that a recurrence relation is exact if it originates from a composition of area preserving twist maps, see Remark 2.2. The main example in our context is when the orientation reversing twist map f is area preserving. Setting $W(\mathbf{u}) = \sum_{i=1}^{d} S_i(u_i, u_{i+1})$ the corresponding parabolic flow is a gradient flow: $\frac{d\mathbf{u}}{dt} = \nabla W$. This implies that invariant sets consists of fixed points and connecting orbits only. The second order character of the recurrence relation leads to the following strong result (see [**15**, section 7]): for an exact parabolic flow on a bounded proper relative braid class $[\mathbf{u} \text{ REL } \mathbf{v}]$, the number of fixed points is bounded below by the number of distinct nonzero monomials in the characteristic polynomial $CP_t(\mathbf{u} \text{ REL } \mathbf{v})$.

EXAMPLE 3.9. We calculate the homotopy index of the braid shown at the left in Figure 7. It is of period two and it is proper and bounded. A braid can evolve only in such a way as to decrease the number of intersections (cf. Proposition 3.4 and Figure 5). Hence along the flow the free anchor point u_0 cannot cross the anchor points of skeleton since this would lead to an increased number of crossing, i.e., u_0 is "trapped" between anchor points of the skeleton. On the other hand, the middle point u_1 of the free strand can evolve in such a way that it crosses the nearest anchor points, since this decreases the number of crossings. Of course, on crossing the anchor point of the skeleton, the free strand leaves the braid class. The configuration space and the flow on the boundary are shown in the middle in Figure 7. The exit set N^- consists of the top and bottom boundaries. The homotopy index of this braid class is $[N/N^-] \simeq (S^1, \mathrm{pt})$, hence $CP_t = t$ and any parabolic flow leaving $\mathbf{v}$ invariant has at least one fixed point inside the braid class.

4. Period-4 points for orientation reversing twist maps

We now apply the theory of braids and parabolic flows to orientation reversing twist maps. Let f be an orientation reversing twist map. As explained in the introduction and Section 2 we can write it as the composition of four orientation preserving twist maps. This leads to a parabolic recurrence relation $\mathcal{R} = (\mathcal{R}_i)_{i\in\mathbb{Z}}$ which is 4-periodic: $\mathcal{R}_{i+4} = \mathcal{R}_i$. Lemma 2.4 gives the correspondence between trajectories of f and solutions of the recurrence relation via the flip transformation (4).

Suppose now that $\{(x^i, y^i)\}_{i=1}^4$ is a period-4 orbit of f, i.e., its minimal period is four. Let $x = \{x^i\}_{i\in\mathbb{Z}}$, then the flipped sequence $\lambda(x)$ is a solution of the recurrence relation $\mathcal{R} = 0$. Obviously, any shift $\sigma^\alpha(x)$ of the sequence x corresponds to the same period-4 orbit of f. Hence $\lambda(\sigma^\alpha(x))$ for $\alpha = 1, 2, 3, 4$ are four solutions of the parabolic recurrence relation $\mathcal{R} = 0$, labeled $\mathbf{v}^1, \mathbf{v}^2, \mathbf{v}^3, \mathbf{v}^4$ respectively, and they thus form the four stationary strands of a closed discretized braid diagram $\mathbf{v} = \{\mathbf{v}^\alpha\} \in \mathcal{D}_4^4$. A priori $\mathbf{v}$ is only in $\overline{\mathcal{D}}_4^4$, but if $\mathbf{v} \in \Sigma$, then necessarily $\mathbf{v} \in \Sigma^-$, since Proposition 3.4 implies there are no stationary points of a parabolic flow on $\Sigma \setminus \Sigma^-$. On the other hand, if $\mathbf{v} \in \Sigma^-$, then at least two of the strands $\lambda(\sigma^\alpha(x))$ coincide, hence the minimal period is smaller than four. However, we are assuming that the initial orbit is a true period-4 orbit and hence the corresponding braid diagram $\mathbf{v}$ is a discretized braid in $\mathcal{D}_4^4$.

The next question is: which braid classes do these period-4 orbits represent? Because we need to make sure that we consider all possible cases, we start simply from the quadruple

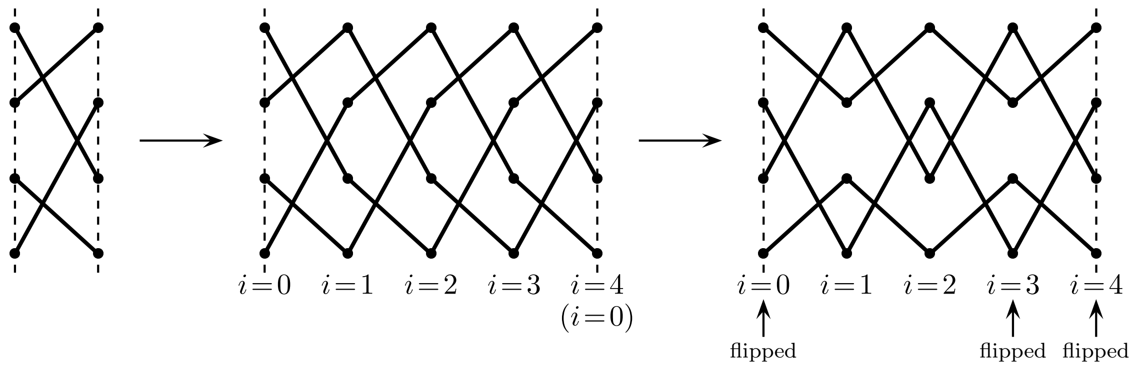

FIGURE 8. Starting from an ordering of the points (x^0, x^1, x^2, x^3) on the left (f permutes the ordered points), one uses four iterates (middle) and then applies the flip (i.e. inverting the order at the zeroth and third coordinates) to obtain the *braid diagram* on the right.

(x^0, x^1, x^2, x^3). Assume, without loss of generality, that $x^0 = \min\{x^i\}$. There are six non-degenerate orderings (degenerate ones are discussed below), namely

$$\begin{aligned} &x^0 < x^1 < x^2 < x^3, \qquad && x^0 < x^1 < x^3 < x^2, \qquad && x^0 < x^2 < x^1 < x^3, \\ &x^0 < x^2 < x^3 < x^1, && x^0 < x^3 < x^1 < x^2, && x^0 < x^3 < x^2 < x^1. \end{aligned} \tag{7}$$

For each of these six possibilities the procedure described above leads to a closed discretized braid diagram. The easiest way to do this is depicted in Figure 8. Namely, one draws the four iterates of the four shifts of the periodic solution. Then one inverts the order of the points at the zeroth and third coordinates to obtain a *braid diagram.* It is perhaps good to point out that the picture in the middle of Figure 8, i.e. before the flip, is *not* interpreted as a braid diagram, since it is not related to a parabolic flow. For the six possible orderings the resulting braid diagrams are shown shown in Figure 9.

The six discretized braid diagrams can be grouped in two distinct topological braid classes, type I and type II, see Figure 9. We note that they are in four distinct discretized braid classes in $\mathcal{D}^4_4$, but on the topologically level these reduce to two classes. Type I has (periodic) braid word $\sigma_2^2\sigma_1^2\sigma_3^2\sigma_2^2\sigma_1^2\sigma_3^2$ and corresponds to orderings $x^0 < x^3 < x^1 < x^2$ and $x^0 < x^1 < x^3 < x^2$, while the (periodic) braid word of type II is $\sigma_1^2\sigma_2\sigma_1^2\sigma_2\sigma_3^2\sigma_2\sigma_3^2\sigma_2$.

As discussed above, since the braid consists of stationary solutions of a parabolic flow, the braid cannot have tangencies. Of course, anchor points can nevertheless coincide, which corresponds to a degenerate case in the ordering of the quadruple x^0, x^1, x^2, x^3. That is, some

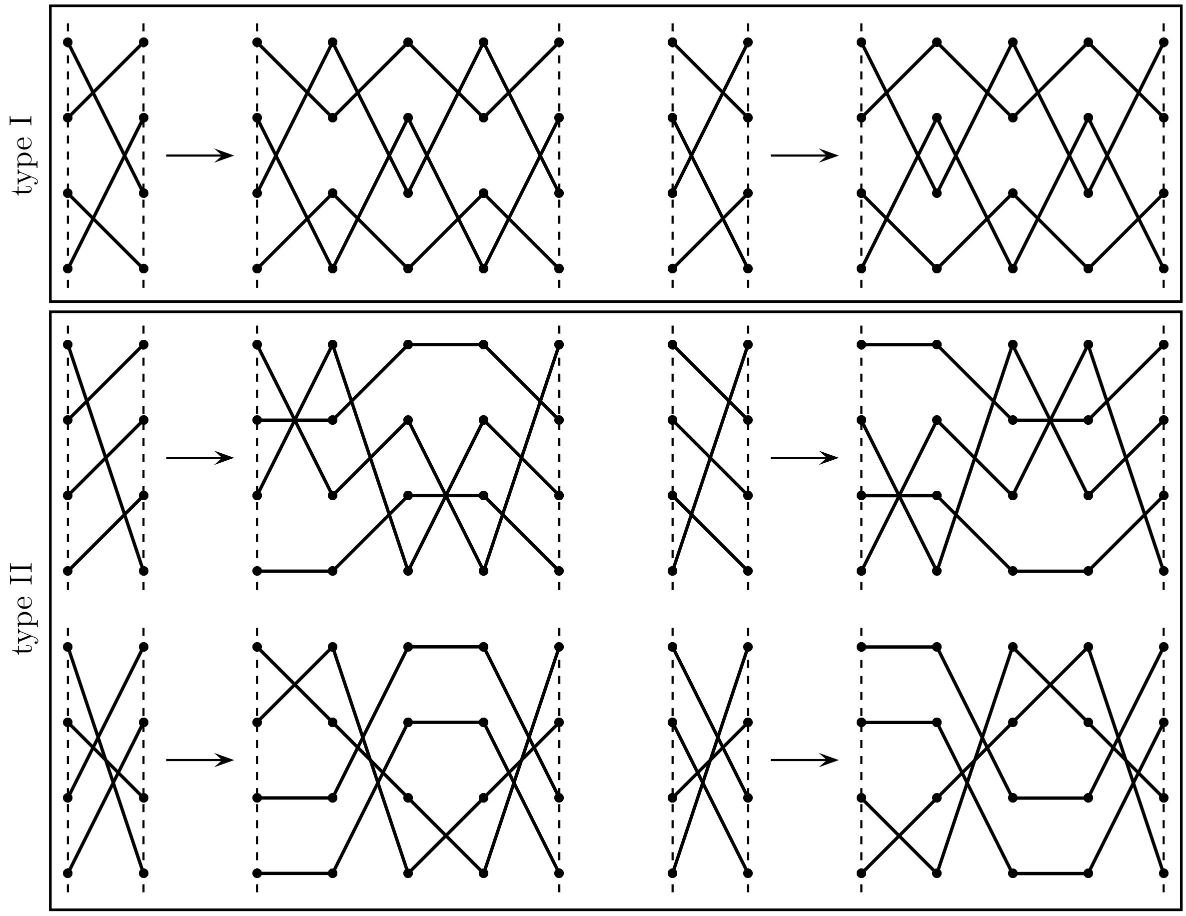

FIGURE 9. The six period-4 orbits and their corresponding braid diagrams.

of the inequalities in (7) are replaced by equalities. Since tangencies in the braid diagram are excluded and since we start from a true period-4 orbit, the only possible degenerate cases turn out to be

$$x^0 < x^1 = x^2 < x^3 \qquad \text{and} \qquad x^0 < x^2 = x^3 < x^1,$$

which both lead to a braid of type II.

REMARK 4.1. The fact that we have four different discretized braid diagrams but only two topological braid classes may lead to notational difficulties that we clarify here while we are at it. The two discretized braid classes within one topological braid class are related by a shift σ or a double shift σ^2. We can thus go back and forth between the two by applying shifts to both $\mathbf{v}$ and $\mathcal{R}$. When we obtain results for a parabolic flow generated by $\mathcal{R}$ that has stationary braid $\mathbf{v}$, then these results carry over to $\sigma(\mathcal{R})$ and $\sigma(\mathbf{v})$, since $\sigma(\mathcal{R})$ is a parabolic recurrence relation that fixes $\sigma(\mathbf{v})$. We may thus restrict our attention to just one of the discretized braid classes in each topological braid class.

5. Positive topological entropy

We are ready to assemble the machinery previously presented in order to prove that a twist map with a period-4 point of type I is chaotic. Throughout this section we assume the infinite twist condition (2), which leads to a proof of Theorem 1.3, see Section 7 for the case of a diffeomorphism. We will show that for f there exists a compact invariant set $\Lambda \subset \mathbb{R}^2$ on which f has positive topological entropy.

Our strategy is to first consider the second iterate f^2 and to show that there is a compact set $\Lambda_1 \subset \mathbb{R}^2$, invariant under f^2, on which it is semi-conjugate to the shift map on three symbols, which has positive entropy. Standard results about the entropy then imply that the map f also has positive entropy on $\Lambda = \Lambda_1 \cup f(\Lambda_1)$. The set of all sequences on three symbols is denoted by $\Sigma_3 = \{-1, 0, +1\}^{\mathbb{Z}}$, and $\sigma\colon \Sigma_3 \to \Sigma_3$ maps $\{a_n\}_{n\in\mathbb{Z}}$ to the shifted sequence $\{a_{n+1}\}_{n\in\mathbb{Z}}$.

Let $\overline{z}$ be a period-4 point of type I. According to Section 4 this means that we may assume that the x-coordinates of its orbit, denoted by $x^i = \pi_x f^i(\overline{z})$, are ordered in a certain way. In particular, in view of Remark 4.1 and considering an iterate of $\overline{z}$ if necessary, we may without loss of generality assume that

$$x^0 < x^3 < x^1 < x^2.$$

Let $S \subset \mathbb{R}^2$ be the set of all complete orbits of f and define

$$\Lambda_1 \stackrel{\text{def}}{=} \{\, z \in S \mid \pi_x f^{2i}(z) \in [x^0, x^2] \text{ and } \pi_x f^{2i+1}(z) \in [x^3, x^1] \text{ for all } i \in \mathbb{Z}\,\}. \tag{8}$$

Remark 2.1 shows that f^{-1} is well-defined (at least on the image of f). We note that $\overline{z}$ and $f^2(\overline{z})$ are elements of Λ_1. The set Λ_1 is invariant under f^2 and it is bounded. By definition the x-coordinates are uniformly bounded on Λ_1, while boundedness of the y-coordinate follows from the fact that the functions $Y(x, x')$ and $\widetilde{Y}(x, x')$ from Section 2 are continuous on $\mathbb{R}^2$ and thus bounded on bounded sets. Furthermore, since f and f^{-1} are continuous (differentiable) functions it is not hard to see that Λ_1 is compact.

Let $\varphi : \Lambda_1 \to \Sigma_3$ be the function that assigns a symbol sequence to each point in Λ_1 as follows:

$$\varphi(z) = \{a_n\}_{n\in\mathbb{Z}} \quad \Longleftrightarrow \quad \begin{cases} a_n = +1 & \text{if } \pi_x f^{2n}(z) \in (x^1, x^2], \\ a_n = 0 & \text{if } \pi_x f^{2n}(z) \in [x^3, x^1], \\ a_n = -1 & \text{if } \pi_x f^{2n}(z) \in [x^0, x^3). \end{cases} \tag{9}$$

The sequence $\{a_n\}_{n\in\mathbb{Z}}$ will be called the symbolic description of a point (trajectory) in Λ_1. We note that

$$\varphi(\overline{z}) = \{(-1)^{n-1}\}_{n\in\mathbb{Z}} \qquad \text{and} \qquad \varphi(f^2(\overline{z})) = \{(-1)^n\}_{n\in\mathbb{Z}}. \tag{10}$$

Our goal is to show that φ is a semi-conjugacy. It follows from the construction that $\varphi \circ f^2(z) = \sigma \circ \varphi(z)$ for all $z \in \Lambda_1$. We still need to show that φ is surjective and continuous. Continuity is proved in Lemma 5.4, while surjectivity follows from Lemma 5.3. Leading up to that we first state and prove the crucial lemma, which uses the concepts of the flip transformation, braid diagrams and their Conley index.

Lemma 5.1. *For any periodic symbol sequence $\{a_n\}_{n\in\mathbb{Z}} \in \Sigma_3$ there exists a point in Λ_1 that has $\{a_n\}_{n\in\mathbb{Z}}$ as its symbolic description.*

Proof. Let p be the minimal period of the sequence $\{a_n\}_{n\in\mathbb{Z}}$, and let $4q$ denote the smallest common multiple of $2p$ and 4.

Step 1. Construction of relative braid classes.
In Section 4 we explained in detail how a period-4 point yields a braid $\mathbf{v} \in \mathcal{D}_4^4$ that is stationary for the parabolic flow associated to the recurrence relation $\mathcal{R} = (\mathcal{R}_i)_{i\in\mathbb{Z}}$. In this section $\mathbf{v}$ is assumed to be a type I braid. By concatenating $\mathbf{v}$ (just repeating it) we obtain more stationary skeletons. To be precise, define $\#_q\mathbf{v}$ to be the q-concatenation of $\mathbf{v}$. Clearly $\#_q\mathbf{v} \in \mathcal{D}_{4q}^4$, and it is a stationary skeleton for $\mathcal{R}$ (cf. Figure 10).

Using the skeletons $\#_q\mathbf{v}$ we can now construct numerous relative braid classes by weaving in a free strand with the skeletal strands. Given a periodic symbol sequence $\{a_n\}$, a free strand $\mathbf{u} = (u_i)_{i=0}^{4q-1}$ can be characterized as follows:

(i) For i odd, $u_i \in (x^3, x^1)$ when $i = 1 \bmod 4$, and $u_i \in (-x^1, -x^3)$ when $i = 3 \bmod 4$.

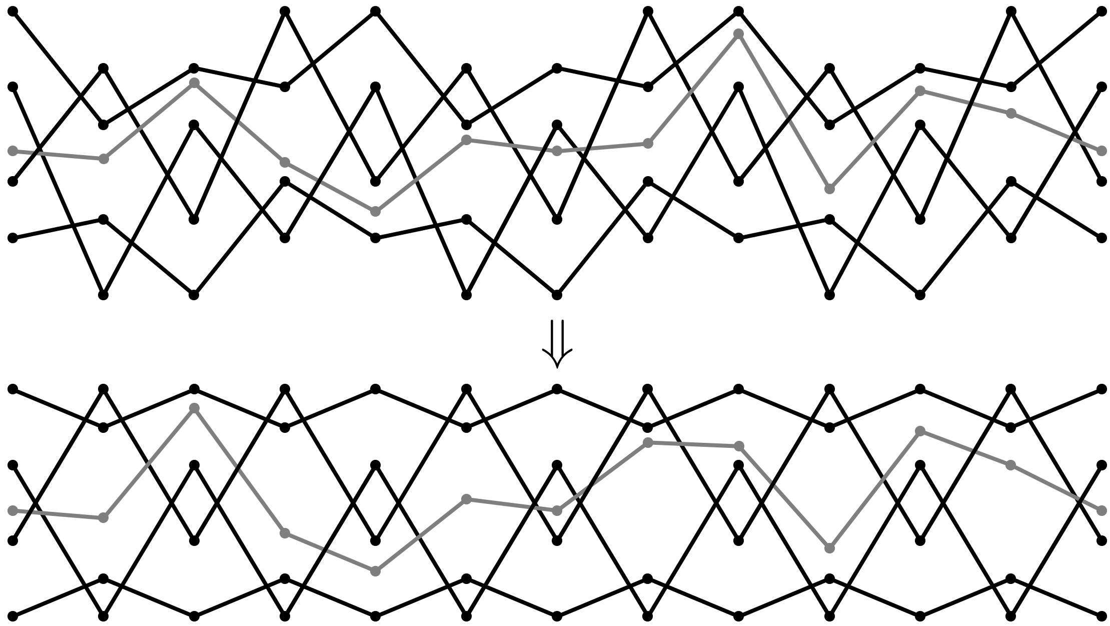

FIGURE 10. Braid diagrams corresponding to $\{\ldots, a_0, a_1, a_2, a_3, a_4, a_5, a_6, \ldots\} = \{\ldots, 0, +1, +1, 0, -1, +1, 0, \ldots\}$. At the top is a generic non-symmetric situation, while at the bottom the skeleton is deformed into a symmetric one, which has the same topological information and has the advantage that it is a lot easier to survey. The homotopy type of this braid class is the pointed space (S^2, pt).

(ii) The position of the even anchors is determined by the sequence $\{a_n\}_{n=0}^{2q-1}$:

if $a_n = +1$ then $u_{2n} \in (x^1, x^2)$ for n odd, and $u_{2n} \in (-x^2, -x^1)$ for n even;
if $a_n = 0$ then $u_{2n} \in (x^3, x^1)$ for n odd, and $u_{2n} \in (-x^1, -x^3)$ for n even;
if $a_n = -1$ then $u_{2n} \in (x^0, x^3)$ for n odd, and $u_{2n} \in (-x^3, -x^0)$ for n even.

Moreover, let $u_{4q} = u_0$. The subdivision of the range of n (basically $n = 0, 3 \bmod 4$ and $n = 1, 2 \bmod 4$) is needed since we are working with the (flipped) coordinates for parabolic recurrence relations. Figure 10 shows an example of a relative braid class obtained in this way. Denote the equivalence class of the relative braids described above by $[\mathbf{u} \text{ REL } \#_q \mathbf{v}]$. If $a_n \not\equiv \pm(-1)^n$, then the these braid classes are bounded and proper. For the sequences $a_n \equiv \pm(-1)^n$ the corresponding points in Λ_1 are given by (10), and we will exclude these special sequences from our considerations.

Step 2. Non-triviality of the Conley index.

We now calculate the Conley index for the braid classes described in step 1. Since each coordinate u_i can only move in the designated intervals as described above, the configuration space $N = \mathrm{cl}([\mathbf{u} \text{ REL } \#_q\mathbf{v}])$ is a cartesian product of intervals, i.e. $N \simeq I^{4q}$, a $4q$-dimensional hypercube. We now proceed by determining N^-, the exit set. As in Example 3.9 the flow can only decrease the total number of intersections if $u_{2n} \in (x^3, x^1)$ or $u_{2n} \in (-x^1, -x^3)$. Then the number of intersections decreases when u_{2n} moves through the boundary of these intervals. The number of anchor points for which this is possible is equal to the number of zeroes in $\{a_n\}_{n=0}^{2q-1}$. Denote this number by k. This way N^- consists only of opposite faces. Therefore, $h = [N/N^-] \simeq (S^k, \mathrm{pt})$. A standard result from homology theory then shows that

$$H_*(N, N^-) = H_*((S^k, \mathrm{pt})) = \begin{cases} \mathbb{R} & \text{if } * = k, \\ 0 & \text{otherwise,} \end{cases}$$

and $CP_t(h) = t^k$, proving that the Conley index is non-trivial for any periodic symbol sequence $\{a_n\}$ with $a_n \not\equiv \pm(-1)^n$. Such symbol sequences will be earmarked as non-trivial.

Step 3. Existence of periodic points.

From the previous step we have that $CP_{-1}(h) = (-1)^k \neq 0$. Lemma 3.7 then proves that there exists at least one stationary point, i.e. a solution of $\mathcal{R} = 0$, in the relative braid class $[\mathbf{u} \text{ REL } \#_q\mathbf{v}]$ that is associated to each of the non-trivial periodic symbol sequences $\{a_n\}$. The considerations in Section 2, in particular Lemma 2.4, imply that the stationary solution $\mathbf{u}$ constructed this way corresponds to a periodic point of f. Hence it corresponds to a $2q$ periodic orbit of f^2 and the construction of the braid classes ensures that this periodic orbit is in Λ_1 and has symbolic description $\{a_n\}$. □

The proof of Lemma 5.1 does not show that every periodic symbol sequences of minimal period p corresponds to a periodic trajectory with period p of f^2 (only when p is even this is clear). Nor do we obtain uniqueness of points in Λ_1 that have a particular periodic symbolic description. However, since we are only building a *semi*-conjugacy, neither of these points matter.

Remark 5.2. For any $z \in \Lambda_1$ the x-coordinates of the even iterates cannot be on the boundary of the intervals distinguishing the different symbolic descriptions, i.e. $\pi_x f^{2n}(z) \neq x^1, x^3$. Namely, suppose $\pi_x f^{2n}(z) = x^1$ or x^3, then after applying the flip transformation and interpreting the flipped trajectory of z as a strand in the braid diagram (see Figure 10), this strand is stationary and has a tangency at anchor point $2n$ with one of the strands of the skeleton. This is impossible, as stated in Proposition 3.4. An alternative is to compare the trajectories of z and $\overline{z}$ and to use the twist property of the orientation reversing twist map f to obtain a contradiction directly.

The periodic symbol sequences from Lemma 5.1 allow us to deal with the general case.

LEMMA 5.3. *For any sequence* $\{a_n\}_{n\in\mathbb{Z}} \in \Sigma_3$ *there exist a point in* Λ_1 *that has* $\{a_n\}_{n\in\mathbb{Z}}$ *as its symbolic description.*

PROOF. Let $a = \{a_n\}_{n\in\mathbb{Z}}$ be any sequence in Σ_3. We can approach a by periodic sequences $a^k \in \Sigma_3$, where $a^k_n = a_n$ for $|n| \leq k$ with periodic extension $a^k_n = a^k_{n-2k-1}$ for all n. Clearly $a^k \to a$ as $k \to \infty$, with a^k being periodic (the metric is given explicitly in the proof of the next lemma). Lemma 5.1 shows that there exist points $z_k \in \Lambda_1$ such that $\varphi(z_k) = a^k$. Since Λ_1 is compact, there exists a convergent subsequence $z_{k_m} \to z \in \Lambda_1$ as $m \to \infty$. Let $\varphi(z) = b \in \Sigma_3$, then we claim that $b = a$. For any fixed $n \in \mathbb{Z}$, $\pi_x f^{2n}(z)$ is either in $[x^0, x^3)$, (x^3, x^1) or $(x^1, x^2]$, because the values x^1 and x^3 are excluded by Remark 5.2. Hence it follows that for m sufficiently large $\pi_x f^{2n}(z_{k_m})$ is in the same of these intervals as $\pi_x f^{2n}(z)$. Since the intervals encode the symbolic description, this implies $b_n = a^{k_m}_n$ for sufficiently large m, and thus indeed $b = a$. $\square$

LEMMA 5.4. *The map* φ *defined in* (9) *is continuous.*

PROOF. The arguments resemble the ones used in the previous proof. We use the metric $d(a, b) = 2^{-\max\{m|a_n=b_n \text{ for } |n|<m\}}$ on Σ_3. Let z_k be any convergent sequence in Λ_1, $z_k \to z \in \Lambda_1$. Let $\varphi(z) = b \in \Sigma_3$ and $\varphi(z_k) = b^k$. For any fixed $n \in \mathbb{Z}$, $\pi_x f^{2n}(z)$ is either in $[x^0, x^3)$, (x^3, x^1) or $(x^1, x^2]$, because the values x^1 sand x^3 are excluded by Remark 5.2. Hence it follows that for k sufficiently large $\pi_x f^{2n}(z_k)$ is in the same of these intervals as $\pi_x f^{2n}(z)$, which implies $b_n = b^k_n$ for sufficiently large k. In particular, for any (large) $m \in \mathbb{N}$ there exists a $K(m) \in \mathbb{N}$ such that $b_n = b^k_n$ for all $|n| \leq m$ and $k \geq K$. In other words, $|\varphi(z) - \varphi(z_k)| \leq 2^{-m-1}$ for $k \geq K$, which establishes continuity. $\square$

From the previous lemmas we conclude that φ as defined by (9) is a semi-conjugacy from $f^2|_{\Lambda_1}$ to $\sigma|_{\Sigma_3}$. To carry over this information to the map f we define

$$\Lambda \stackrel{\text{def}}{=} \Lambda_1 \cup f(\Lambda_1),$$

which is invariant under f, and the entropy of f on Λ can be estimated in terms of the entropy of the shift on three symbols.

THEOREM 5.5. *An orientation reversing twist map of the plane that satisfies the infinite twist condition and that has a type I period-4 point, has positive topological entropy restricted to the compact invariant set* Λ.

PROOF. We use the semi-conjugacy φ to estimates the entropy $h(f|_\Lambda)$ of f on Λ. Standard properties of the entropy (e.g. see [**13**]) give the estimates

$$h(f|_\Lambda) = \frac{1}{2}h(f^2|_\Lambda) \geq \frac{1}{2}h(f^2|_{\Lambda_1}) \geq \frac{1}{2}h(\sigma|_{\Sigma_3}) = \frac{1}{2}\ln(3).$$

□

REMARK 5.6. As an alternative strategy one can consider the fourth iterate of f instead of the second one. This is perhaps more natural in view of the decomposition of f^4 in terms of orientation preserving twist maps, as discussed in the introduction. On the other hand, the notation becomes a bit more involved. Anyway, it is not difficult to see that arguments analogous to the ones used for the second iterate lead to a semi-conjugacy of $f^4|_{\Lambda_1}$ to the shift on the space Σ_9 of sequences on nine symbols. This approach gives exactly the same lower bound for the topological entropy of f:

$$h(f|_\Lambda) \geq \frac{1}{4}h(f^4|_{\Lambda_1}) \geq \frac{1}{4}h(\sigma|_{\Sigma_9}) = \frac{1}{4}\ln(9) = \frac{1}{2}\ln(3).$$

6. Type II periodic points

In the previous section we have proved that a period-4 orbit of type I forces orientation reversing twist maps to be chaotic. Now we will show that the theorem is "sharp" in the sense that we construct an example of a map with a period-4 orbit of type II that has zero topological entropy, i.e., the entropy of the dynamics restricted to any bounded invariant set is zero.

We start with the well known quadratic family of one dimensional maps

$$x_{k+1} = \lambda x_k(1 - x_k),$$

where λ is a parameter. This map is a good starting point since it has a simple formula and its dynamics has been studied extensively. The property of most interest to us is that for λ slightly larger than

$$\lambda^* = 1 + \sqrt{6},$$

the system has a period-4 orbit which is stable (the period-2 orbit undergoes a period doubling bifurcation at $\lambda = \lambda^*$). Moreover, the topological entropy of the map on the maximal bounded invariant set is zero.

We want to embed this system into $\mathbb{R}^2$ and turn it into an orientation reversing twist map. To accomplish this we use the family of maps

$$f_\varepsilon : \begin{pmatrix} x \\ y \end{pmatrix} \to \begin{pmatrix} y \\ \varepsilon x + \lambda y(1-y) \end{pmatrix},$$

which are orientation reversing twist diffeomorphisms for all $\varepsilon > 0$, while for $\varepsilon = 0$ we retrieve the quadratic family in disguise (f_0 is *not* a diffeomorphism). Notice that for $\varepsilon = 0$, and λ slightly larger than λ^*, the period-4 orbit is of type II (cf. Section 4). Intuition suggests that for small $\varepsilon > 0$ the perturbation εx will not change the dynamics much (in particular, the entropy remains zero). The remainder of this section is spent on making this precise.

Since our aim is to show that the maps for $\varepsilon > 0$ have zero topological entropy we prove that their non-wandering sets are all "the same", and in a sense "copies" of the non-wandering set at $\varepsilon = 0$, i.e., we will prove a version of Ω-stability for this particular situation. Let S^ε be the set of all all points in $\mathbb{R}^2$ through which there is a complete bounded orbit of f_ε, and let Ω^ε be the set of non-wandering points of f_ε. We start with proving that all interesting dynamics is contained in the compact set $N \stackrel{\text{def}}{=} [-1, 2] \times [-1, 2]$.

LEMMA 6.1. *For $\varepsilon \in [0, 1/2)$ and $\lambda \in [1, 4]$ it holds that $\Omega^\varepsilon \subset S^\varepsilon \subset \mathrm{int}(N)$.*

PROOF. The case $\varepsilon = 0$ corresponds to the one-dimensional quadratic map and the statements are easily seen to hold. We turn to the case $\varepsilon \in (0, 1/2)$, for which f_ε is invertible. First we show that $S^\varepsilon \subset N$. Let us start with the bound $x_n, y_n < 2$. By contradiction, assume that $x_0 \geq 2$, then since $\lambda y_n(1-y_n) \leq 1$ we have

$$x_{n-2} \geq \frac{x_n - 1}{\varepsilon}.$$

Hence the sequence $x_{-2k} \to \infty$, as $k \to \infty$. This contradicts the fact that trajectory is bounded, so indeed $x_n < 2$ for all n. Since $y_n = x_{n+1}$ we then also have $y_n < 2$.

Next we prove that $x_n, y_n > -1$. If $y_0 \leq -1$ then the inequality

$$y_{n+1} < \lambda y_n(1-y_n) + 1$$

implies that $y_k \to -\infty$ as $k \to \infty$. Therefore $y_n > -1$ and again the same holds for x_n.

We now show that also $\Omega^\varepsilon \subset N$. From the previous argument we see that if this is not the case then there has to be some point $(x_0, y_0) \in \Omega^\varepsilon$ for which $x_0 \geq 2$. It then follows that $x_{-2k} \to \infty$, and since x_0 is non-wandering x_{-2m+1} has to be arbitrarily close to $x_0 \geq 2$ for some $m \in \mathbb{N}$. The same reasoning as before then shows that $x_{-2m+1-2k} \to \infty$ as $k \to \infty$, contradicting the fact that $(x_0, y_0) \in \Omega^\varepsilon$. We have thus established that $\Omega^\varepsilon \subset N$. Finally, if $z \in \Omega^\varepsilon$, then $f_\varepsilon(z) \in \Omega^\varepsilon$ and $f_\varepsilon^{-1}(z) \in \Omega^\varepsilon$, hence $\Omega^\varepsilon \subset S^\varepsilon$. □

In Ω-stability theory the concept of axiom A maps and the no-cycle property are usually essential (see for example [**24**]). Let us recall their standard definitions. For a compact manifold M, we say that a map $f : M \to M$ satisfies *axiom A* if the set $\Omega(f)$ is hyperbolic and the periodic points are dense in $\Omega(f)$. When f satisfies axiom A then the non-wandering set $\Omega(f)$ can be written as a finite disjoint union $\Omega = \Omega_0 \cup \cdots \cup \Omega_k$ of closed invariant sets on which f is topologically transitive (the spectral decomposition theorem, cf. [**24**]). The sets Ω_i are called basic sets. We say that $\Omega_i \leq \Omega_j$ if $(W^s(\Omega_i) \setminus \Omega_i) \cap (W^u(\Omega_j) \setminus \Omega_j) \neq \varnothing$, where the stable and unstable sets are given by

$$W^s(\Omega_i) = \{x \in M \mid f^n(x) \to \Omega_i \text{ as } n \to \infty\}$$
$$W^u(\Omega_i) = \{x \in M \mid f^{-n}(x) \to \Omega_i \text{ as } n \to \infty\}.$$

A map f satisfying axiom A has the no-cycle property if for every choice of distinct indices $\{i_k\}_{k=1}^n$, $n \geq 1$ it is impossible to have the inequalities

$$\Omega_{i_1} \leq \Omega_{i_2} \leq \ldots \leq \Omega_{i_n} \leq \Omega_{i_1}.$$

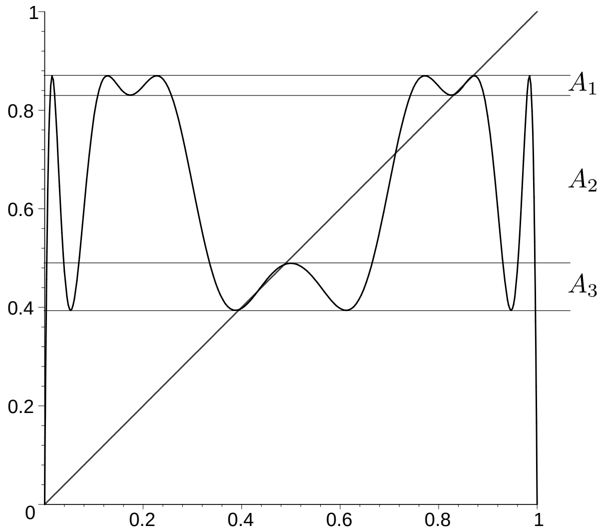

FIGURE 11. The graph of the fourth power of the quadratic map. The parameter λ is set to $\lambda^* + 0.04$. The intervals A_1, A_2 and A_3 (bounded by the extrema) are indicated.

Since our case does not fit in the usual setting of diffeomorphisms on a compact manifold we will now adapt these concepts to the family f_ε. For f_0 the invariant set is

$$S^0 = \{(x, y) \mid x \in [0, \lambda/4] \text{ and } y = \lambda x(1 - x)\}.$$

For values of λ slightly larger than λ^* there are two unstable fixed points, an unstable period-2 orbit and stable period-4 orbit. For simplicity we write

- Ω_1 – period-4 orbit;
- Ω_2 – period-2 orbit;
- Ω_3 – non-trivial fixed point;
- Ω_4 – fixed point $(0, 0)$.

We would like to show that these are the only non-wandering points. To analyze the dynamics we observe that for the fourth power F_λ^4 of quadratic map $F_\lambda(x) = \lambda x(1-x)$ eventually maps any point $x_0 \in (0, 1)$ into the interval $A = [F_\lambda(\lambda/4), \lambda/4]$ (cf. Figure 11). On the other hand, in A we can distinguish three intervals $A_1 = [F_\lambda(\lambda/4), F_\lambda^3(\lambda/4)]$, $A_2 = (F_\lambda^3(\lambda/4), F_\lambda^2(\lambda/4))$ and $A_3 = [F_\lambda^2(\lambda/4), \lambda/4]$. Monotonicity of F_λ^4 on $A_2 \cap (F_\lambda^4)^{-1}(A_2)$ guarantees that any point in A, with the exception of the fixed point Ω_2, will eventually enter A_1 or A_3 under iterates of F_λ^4. Apart from the period-2 orbit any point in A_1 and A_3 approaches the period-4 orbit due to monotonicity of F_λ^4 on these intervals (cf. Figure 12). Our choice of λ is sufficiently

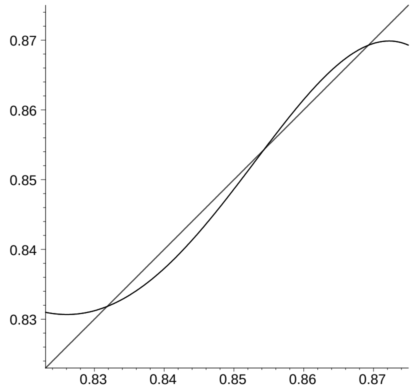

FIGURE 12. One of the two trapping regions of the period-4 orbit. We choose λ so close to λ^* that the function is monotone between the three fixed points of F_λ^4 in the picture.

close to λ^* so that the function F_λ^4 is monotone between the three fixed points of F_λ^4 in A_1 and A_3. Since f_0 mimics the dynamics of F_λ, it follows that any point in S^0 that is not eventually periodic has Ω_3 as its ω-limit set. Moreover, we have proved that there are no other non-wandering points then the orbits contained in Ω_i for $i = 1, 2, 3, 4$, i.e.

$$\Omega^0 = \Omega_1 \cup \Omega_2 \cup \Omega_3 \cup \Omega_4.$$

One can easily see that the eigenvalues of df_0 in a point in Ω^0 are $\alpha_1 = 0$ and α_2, which is equal to the eigenvalue of the corresponding point of F_λ. Again, since for λ sufficiently close to λ^*, and $\lambda > \lambda^*$, we have $F_\lambda' \neq \pm 1$ at the fixed points, the period-2 and the period-4 orbit. Hence, they are all hyperbolic, and Ω_i is hyperbolic for $i = 1, 2, 3, 4$.

The reasoning above shows that f_0 has a hyperbolic non-wandering set which only consists of periodic orbits. Moreover, we have identified the basic sets to be Ω_i with $i = 1, 2, 3, 4$. Now we turn to the no-cycle property. To simplify the notation we write $\widetilde{W}^s(\Omega_i) = W^s(\Omega_i) \setminus \Omega_i$ and $\widetilde{W}^u(\Omega_i) = W^u(\Omega_i) \setminus \Omega_i$. To exclude the existence of a cycle let us start with the observation that $\widetilde{W}^s(\Omega_4) \cap S^0 = \varnothing$. This ensures that $\Omega_i \not\lesssim \Omega_4$ for $i = 1, 2, 3, 4$. On the other hand $\widetilde{W}^u(\Omega_1) = \varnothing$, so $\Omega_1 \not\lesssim \Omega_i$ for $i = 1, 2, 3, 4$. From the arguments above (illustrated in Figures 11 and 12) it follows that $\widetilde{W}^u(\Omega_3) \subset W^s(\Omega_1) \cup W^s(\Omega_2)$ and $\widetilde{W}^u(\Omega_2) \subset W^s(\Omega_1)$. Combining these observation we see that there are no cycles among $\{\Omega_i\}_{i=1}^4$. This reasoning shows that

LEMMA 6.2. *For λ slightly larger than λ^* the map f_0 has a finite hyperbolic non-wandering set, and there are no cycles among the basic sets.*

We are now in a position to prove Ω-stability and in particular

LEMMA 6.3. *There exists an ε^* such that for all $\varepsilon \in [0, \varepsilon^*]$ the set Ω^ε is finite.*

PROOF. We will mimic the proof of Ω-stability theorem for diffeomorphisms on a compact set in [**24**]. From the lemmas above we know that $\Omega^0 = \mathrm{per}(f_0) = \Omega_1 \cup \Omega_2 \cup \Omega_3 \cup \Omega_4$. It is well know that for f_0 there exist a Lyapunov function (see [**17**]). So there exists a function $V\colon N \to \mathbb{R}$ satisfying the following conditions. It is decreasing along trajectories of f_0, except on Ω_i, $i = 1, 2, 3, 4$, where V is constant. Furthermore, because of the no-cycle property we may assume that $V(\Omega_i) \neq V(\Omega_j)$ for $i \neq j$. Also, we can rescale V so that $V\colon N \to (\frac{1}{2}, 4\frac{1}{2}]$ and $V(\Omega_i) = i$. We define the (compact) sets

$$M_j \stackrel{\text{def}}{=} V^{-1}((-\infty, j + 1/2]) \cap N.$$

The sets M_j have the properties of a filtration:

(1) $N = M_4 \supset M_3 \supset M_2 \supset M_1 \supset M_0 = \varnothing$;
(2) $f_0(M_j) \subset \mathrm{int}(M_j)$;
(3) $\Omega_j \subset \mathrm{int}(M_j \setminus M_{j-1})$;
(4) $\Omega_j = \bigcap_{k=-\infty}^{\infty} f_0^k(M_j \setminus M_{j-1})$;

where f_0^{-k} denotes the k-th pre-image. These properties follow from the definition of M_j and the structure of Ω^0. For simplicity denote

$$U_j \stackrel{\text{def}}{=} M_j \setminus M_{j-1}.$$

By the continuity of the family f_ε and the compactness of N we can choose ε_1 so small that property (2) holds for all $\varepsilon \leq \varepsilon_1$, i.e. $f_\varepsilon(M_j) \subset \mathrm{int}(M_j)$ for all j.

Since Ω_i consists of a hyperbolic periodic orbit, Ω_i continues under perturbations. The perturbed periodic orbit, denoted by Ω_i^ε, is again hyperbolic for ε sufficiently small, say $\varepsilon \leq \varepsilon_2 \leq \varepsilon_1$. Clearly $\Omega_i^\varepsilon \subset \Omega^\varepsilon$ for all i. To conclude the proof we show the other inclusion $\Omega^\varepsilon \subset \Omega_1^\varepsilon \cup \Omega_2^\varepsilon \cup \Omega_3^\varepsilon \cup \Omega_4^\varepsilon$.

We will prove the two following claims. Firstly, for ε sufficiently small, $\Omega_j^\varepsilon = S^\varepsilon(U_j)$, where $S^\varepsilon(U_j)$ is the set of all points in $\mathbb{R}^2$ whose complete orbits lie entirely in U_j. Secondly, if $z \in \Omega^\varepsilon \cap U_j$ for some $\varepsilon \leq \varepsilon_2$ and some j, then $f_\varepsilon^i(z) \in U_j$ for all $i \in \mathbb{Z}$. Let us assume for the moment that the claims are true for $\varepsilon \leq \varepsilon^* \leq \varepsilon_2$. Let $z_0 \in \Omega^\varepsilon$ for some $\varepsilon \in (0, \varepsilon^*]$. By property (1) of the sets M_j the point z_0 has to be in some U_{j_0}. By the second claim the whole trajectory of z_0 is contained in U_{j_0}. Then the first claim shows that $z_0 \in \Omega_j^\varepsilon$. This proves that the non-wandering set for f_ε consists entirely of the perturbation of the non-wandering set of f_0. In particular, Ω^ε is finite. Now we return to the proof of the claims.

Claim 1: $\Omega_j^\varepsilon = S^\varepsilon(U_j)$ for all j and all ε sufficiently small. Because of property (3) of the set M_j we get $\Omega_j^\varepsilon \subset S^\varepsilon(U_j)$ for ε sufficiently small. For the other inclusion we argue by contradiction. Setting $\varepsilon = 1/n$ we assume that for all $n \geq n_0 \in \mathbb{N}$ there is a $z_n \in S^{1/n}(U_j)$ such that $z_n \notin \Omega_j^{1/n}$. By the hyperbolicity of Ω_j (and Ω_j^ε) there is a $\delta > 0$ such that $f_{1/n}^{k(n)}(z_n)$ is not in a δ-ball $B_\delta(\Omega_j)$ around Ω_j for some $k(n) \in \mathbb{Z}$. Set $w_n = f_{1/n}^{k(n)}(z_n)$, then $w_n \in S^{1/n}(U_j) \setminus B_\delta(\Omega_j)$. By compactness of N there exists a subsequence $m_0(n)$ so that $w_{m_0(n)} \to v_0 \in \overline{U_j} \setminus B_\delta(\Omega_j)$. We want to show that $v_0 \in U_j$ and that there is an complete orbit in U_j through v_0. First we prove that $f_0^i(v_0) \in U_j$ for all $i \geq 0$. If this would not be the case then $f_0^i(v_0) \in M_{j-1}$ for some $i \geq 0$. From the property (2) of the sets M_j we get $f_0^{i+1}(v_0) \in \mathrm{int}(M_{j-1})$, and from the continuity of the family f_ε and the continuity of the map it follows that $f_{1/m_0(n)}^{i+1}(w_{m_0(n)}) \in \mathrm{int}(M_{j-1})$ for n large, which contradicts the assumption that $w_{m_0(n)} \in U_j$. We thus have that $f_0^i(v_0) \in U_j$ for all $i \geq 0$. To get the same for pre-images of v_0 we need to extract further subsequences.

From the sequence $m_0(n)$ we extract yet another subsequence $m_1(n)$ such that $f_{1/m_1(n)}^{-1}(w_{m_1(n)})$ converges to, say, v_{-1}. It easily follows that $f_0(v_{-1}) = v_0$. Similarly, from the sequence $m_1(n)$ we can extract a subsequence $m_2(n)$ such that $f_{1/m_2(n)}^{-2}(w_{m_2(n)}) \to v_{-2}$, and $f_0(v_{-2}) = v_{-1}$. We can repeat this procedure inductively and we end up with a sequence $\{v_k\}_{k=-\infty}^0 \subset \overline{U_j}$ and $f_0(v_{-k}) = v_{-k+1}$. In fact, $v_{-k} \in U_j$ $(k \in \mathbb{N})$, because if $v_{-k} \in \overline{U_j} \setminus U_j$, then $v_{-k+1} = f(v_{-k}) \in \mathrm{int}(M_{j-1})$, a contradiction.

We have now constructed a whole trajectory $\{v_k\}_{k=-\infty}^0 \cup \{f_0^k(v_0)\}_{k=0}^\infty$ of f_0 contained in $S^0(U_j)$. By property (4) of the sets M_j this trajectory has to be contained in Ω_j, but since $v_0 \notin B_\delta(\Omega_j)$ we get a contradiction, which concludes the proof of the claim 1.

Claim 2: For all $z \in \Omega^\varepsilon$ with $\varepsilon \in (0, \varepsilon_2]$ it holds that if $z \in U_j$, then $f_\varepsilon^i(z) \in U_j$ for all $i \in \mathbb{Z}$. It is worth recalling that $\varepsilon \leq \varepsilon_2$ implies that $f_\varepsilon(M_j) \subset \mathrm{int}(M_j)$. Assume that $z \in \Omega^\varepsilon \cap U_j$ for some j.

Firstly, we show that $f_\varepsilon^i(z) \in U_j$ for all $i \geq 0$. Since z is in M_j we know that $f_\varepsilon^i(z)$ is in the interior of M_j for every positive i. Next, $f_\varepsilon^i(z) \notin M_{j-1}$ for all $i > 0$. Namely, if $f_\varepsilon^i(z) \in M_{j-1}$ for some $i > 0$, then the next iterate is in the interior of M_{j-1}. The continuity of the map guarantees that $f_\varepsilon^{i+1}(B_\delta(z)) \subset \mathrm{int}(M_{j-1})$, for δ sufficiently small, which also implies $f_\varepsilon^{i+1+k}(B_\delta(z)) \subset \mathrm{int}(M_{j-1})$ for all $k \in \mathbb{N}$. On the other hand, $B_\delta(z) \cap M_{j-1} = \varnothing$, for sufficiently small δ. Hence, $f_\varepsilon^{i+1+k}(B_\delta(z)) \cap B_\delta(z) = \varnothing$ for all positive k and δ sufficiently small, which contradicts $z \in \Omega^\varepsilon$.

Secondly, we show that also the negative iterates $f_\varepsilon^{-i}(z) \in U_j$, for all $i > 0$. We have to show that $f_\varepsilon^{-i}(z) \notin M_{j-1}$ and that $f_\varepsilon^{-i}(z) \notin U_{j+m}$, where $i, m > 0$. As above it follows that if $f_\varepsilon^{-i}(z) \in M_{j-1}$, then $z = f_\varepsilon^{-i+i}(z) \in \mathrm{int}(M_{j-1})$, whereas $z \in U_j$, which shows that $f_\varepsilon^{-i}(z) \notin M_{j-1}$. To prove that $f_\varepsilon^{-i}(z) \notin U_{j+m}$, $m > 0$, we observe that the non-wandering set Ω^ε is invariant under f_ε and f_ε^{-1}. If we would have that $\tilde{z} = f_\varepsilon^{-i}(z) \in U_{j+m}$ for some $i > 0$ and some $m > 0$, then $\tilde{z} \in \Omega^\varepsilon$ and $f_\varepsilon^k(\tilde{z}) \in U_{j+m}$, for all $k \geq 0$, by the result on positive iterates established above. This contradicts the fact that $f_\varepsilon^i(\tilde{z}) = z \in U_j$, concluding the proof of claim 2 and therefore the lemma. □

We have thus found our counterexample.

LEMMA 6.4. *The orientation reversing twist maps f_ε, with λ slightly larger than λ^* and ε sufficiently small, which have a period-4 orbit of type II, have zero topological entropy (as explained at the beginning of this section).*

PROOF. Lemma 6.3 proves that the non-wandering set Ω^ε of f_ε is finite. Standard results on the topological entropy show that the entropy of f_ε on S^ε is equal to the entropy on Ω^ε, and the entropy of the map on a finite set is zero (e.g. see [**24**]). □

7. Twist diffeomorphisms of the plane

We now extend our results to situations where the parabolic recurrence relation is not defined on the whole of $\mathbb{R}^3$. Since this requires some careful analysis, this section is substantially more technical than the previous ones. We first introduce the necessary frame work and in Section 7.3 we apply it to period-4 orbits of orientation reversing twist diffeomorphisms and we prove Theorem 1.2.

7.1. The domain of parabolic recurrence relations. We are interested in *bijective* orientation reversing twist maps. In the introduction it has been explained that the fourth iterate can be decomposed in four orientation preserving positive twist maps, to which we can apply the theory of parabolic flows. We thus restrict our attention here to orientation *preserving* twist diffeomorphisms, and compositions thereof. We assume f is an orientation preserving twist diffeomorphism, i.e. f is bijective to $\mathbb{R}^2$, $df \neq 0$, and $\partial_2(\pi_x f) > 0$. By definition the function f^{-1} is defined on $\mathbb{R}^2$, it is differentiable by the inverse function theorem, and $\partial_2(\pi_x f^{-1}) < 0$, i.e. f^{-1} has negative twist.

We recall and refine some notation from Section 2. Let $(x', y') = f(x, y)$, then there are differentiable functions Y_f and $\widetilde{Y}_f$ with $\partial_2 Y_f > 0$ and $\partial_1 \widetilde{Y}_f < 0$, such that

$$y = Y_f(x, x') \qquad \text{and} \qquad y' = \widetilde{Y}_f(x, x'). \tag{11}$$

Since f^{-1} has negative twist, the same reasoning as in Section 2 gives differentiable functions $Y_{f^{-1}}$ and $\widetilde{Y}_{f^{-1}}$ with $\partial_2 Y_{f^{-1}} < 0$ and $\partial_1 \widetilde{Y}_{f^{-1}} > 0$, such that $y' = Y_{f^{-1}}(x', x)$ and $y = \widetilde{Y}_{f^{-1}}(x', x)$. Obviously

$$Y_f(x, x') = \widetilde{Y}_{f^{-1}}(x', x) \qquad \text{and} \qquad \widetilde{Y}_f(x, x') = Y_{f^{-1}}(x', x).$$

Let us consider the domain D of Y_f and $\widetilde{Y}_f$, and define

$$g(x) \stackrel{\text{def}}{=} \lim_{y \to -\infty} \pi_x f(x, y) \qquad \text{and} \qquad h(x) \stackrel{\text{def}}{=} \lim_{y \to \infty} \pi_x f(x, y). \tag{12}$$

These are functions from $\mathbb{R}$ to $[-\infty, \infty]$. Since they are limits of monotone sequences of continuous functions, g is upper semi-continuous and h lower semi-continuous, and $g(x) < h(x)$ for all $x \in \mathbb{R}$. The domain of Y_f and $\widetilde{Y}_f$ is the open set given by

$$D = \{(x, x') \mid x \in \mathbb{R},\, g(x) < x' < h(x)\}.$$

When f is invertible we can use the same arguments for f^{-1}. We define $G(x) = \lim_{y \to \infty} \pi_x f^{-1}(x, y)$ and $H(x) = \lim_{y \to -\infty} \pi_x f^{-1}(x, y)$. The domain of $Y_{f^{-1}}$ and $\widetilde{Y}_{f^{-1}}$ is given by $\widetilde{D} = \{(x', x) \mid x' \in \mathbb{R},\, G(x') < x < H(x')\}$. Obviously $(x, x') \in D$ if and only if $(x', x) \in \widetilde{D}$, i.e. $\widetilde{D} = D^{-1}$. This gives us a lot of information on g and h. In fact, the boundary ∂D of D consists of at most four pieces, each of which is a monotone graph. This is depicted in Figure 13.

It takes some notation to make this precise. The function $h : \mathbb{R} \to (-\infty, \infty]$ is lower semi-continuous; there is a point $x_h \in [-\infty, \infty]$ such that $h(x_h) = \infty$ and h is non-decreasing for $x < x_h$, and non-increasing for $x > x_h$. This means that h consists of at most two pieces of real-valued functions on (semi-)infinite intervals, a non-decreasing function h^+ and a non-increasing one h^-. Since h and/or x_h can be infinite, h^- and/or h^+ may be nonexistent.

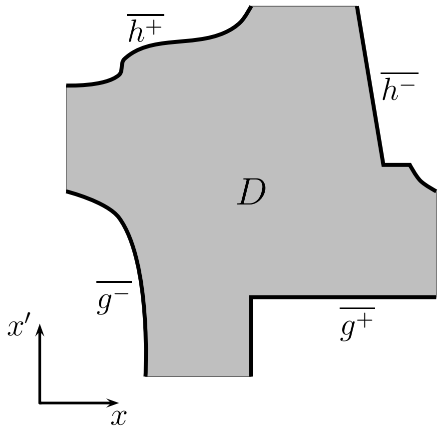

FIGURE 13. The domain D of the functions Y_f and $\widetilde{Y}_f$ for a twist diffeomorphism f.

The associated graphs are

$$\overline{h^\pm} = \mathrm{gr}(h^\pm) = \partial\{(x,x') \in \mathbb{R}^2 \,|\, x \in \mathrm{dom}(h^\pm), x' < h^\pm(x)\} \subset \mathbb{R}^2.$$

In Figure 13 $\overline{h^+}$ is the northwest boundary and $\overline{h^-}$ is the northeast boundary. A similar description is valid for g, with g^+ being non-decreasing (the southeast) and g^- being non-increasing (the southwest). The boundary of $D \subset \mathbb{R}^2$ thus consists of the (at most four) graphs $\overline{g^\pm}$ and $\overline{h^\pm}$.

Since the parabolic recurrence relation, and hence the parabolic flow, is not defined on the boundary ∂D, we need to define (preferably smooth) approximations to it. We construct here the smooth approximations to the northwest boundary $\overline{h^+}$. The other boundaries are dealt with similarly. Let $h^{+\varepsilon}$ be a cutoff/extension function of h^+: $h^{+\varepsilon}(x) = \min\{\varepsilon^{-1}, h^+(x)\}$ for $x \in \mathrm{dom}(h^+)$ and $h^{+\varepsilon}(x) = \varepsilon^{-1}$ for $x \notin \mathrm{dom}(h^+)$. We make it smooth by using a one-sided mollification as follows. Let $z(x)$ be a nonnegative function with support in $[0,1]$ and integral $\int_{\mathbb{R}} z = 1$; let $z_\varepsilon(x) = \varepsilon^{-1} z(x/\varepsilon)$. Define

$$h^+_\varepsilon(x) \;=\; \varepsilon\,\frac{\mathrm{arctanh}(x) - 1}{2} + \int_{\mathbb{R}} z_\varepsilon(y) h^{+\varepsilon}(x-y)\,dy.$$

The ε-approximation h^+_ε of $\overline{h^+}$ is smooth on $\mathbb{R}$. Because of the one-sided mollification and the addition of a small increasing term, h^+_ε is increasing, hence $h^{+\prime}_\varepsilon > 0$, and

$$h^+(x-\varepsilon) - \varepsilon < h^+_\varepsilon(x) < h^+(x) \tag{13}$$

provided $x - \varepsilon \in \mathrm{dom}(h^+)$. This means that $\mathrm{gr}(h_\varepsilon^+)$ is $\sqrt{2}\varepsilon$-close to $\overline{h^+}$ on the piece where $h_\varepsilon^+ < \varepsilon^{-1}$. The cut-off along the x' coordinate will cause no problems since we will only be interested in bounded braid classes, i.e. bounded subset of $\mathbb{R}^2$. Furthermore, h_ε^+ is strictly increasing in ε. It follows from (11), (12) and (13) that

$$\lim_{\varepsilon\to 0} Y(x, h_\varepsilon^+(x)) = \infty \qquad \text{for all } x \in \mathrm{dom}(h^+), \tag{14a}$$

$$\lim_{\varepsilon\to 0} \widetilde{Y}((h_\varepsilon^+)^{-1}(x'), x') = \infty \qquad \text{for all } x' \in \mathrm{range}(\overline{h^+}). \tag{14b}$$

Since we are interested in compositions $f_{d-1} \circ f_{d-2} \circ \cdots \circ f_1 \circ f_0$ of orientation preserving twist maps, we index the corresponding g and h accordingly. The ε-approximation of the domain D_i of Y_i is thus

$$D_{i,\varepsilon} = \{(x_i, x_{i+1}) \,|\, g_{i,\varepsilon}^\pm(x_i) \le x_{i+1} \le h_{i,\varepsilon}^\pm(x_i)\}.$$

7.2. Restricted braid classes. The spaces of *restricted* braid diagrams are defined as (cf. [**15**])

$$\begin{aligned}
\overline{\mathcal{E}}_d^n &\stackrel{\text{def}}{=} \overline{\mathcal{D}}_d^n \cap \{\mathbf{u} \,|\, (u_i^\alpha, u_{i+1}^\alpha) \in D_i \text{ for } i = 0 \dots d-1 \text{ and } \alpha = 1 \dots n\},\\
\mathcal{E}_d^n &\stackrel{\text{def}}{=} \mathcal{D}_d^n \cap \{\mathbf{u} \,|\, (u_i^\alpha, u_{i+1}^\alpha) \in D_i \text{ for } i = 0 \dots d-1 \text{ and } \alpha = 1 \dots n\},\\
\Sigma_{\mathcal{E}} &\stackrel{\text{def}}{=} \overline{\mathcal{E}}_d^n \setminus \mathcal{E}_d^n.
\end{aligned}$$

For $\mathbf{u} \in \mathcal{E}_d^n$ the restricted braid class $[\mathbf{u}]_{\mathcal{E}}$ is defined as $[\mathbf{u}] \cap \mathcal{E}$. For $\mathbf{v} \in \mathcal{E}_d^m$ and $\mathbf{u} \cup \mathbf{v} \in \mathcal{D}_d^{n+m}$ the restricted relative braid class $[\mathbf{u} \text{ REL } \mathbf{v}]_{\mathcal{E}}$ is $[\mathbf{u} \text{ REL } \mathbf{v}] \cap \{\mathbf{u} \in \mathcal{E}_d^n\}$.

The boundary of a restricted relative braid class $[\mathbf{u} \text{ REL } \mathbf{v}]_{\mathcal{E}}$ consists of two parts, namely the singular braids in $\partial[\mathbf{u} \text{ REL } \mathbf{v}]_{\mathcal{E}} \cap \Sigma_{\mathcal{E}}$, and the braids that violate the restriction in $\partial[\mathbf{u} \text{ REL } \mathbf{v}]_{\mathcal{E}} \setminus \Sigma_{\mathcal{E}}$. The parabolic flow is well-defined on $\partial[\mathbf{u} \text{ REL } \mathbf{v}]_{\mathcal{E}} \cap \Sigma_{\mathcal{E}}$ but not on $\partial[\mathbf{u} \text{ REL } \mathbf{v}]_{\mathcal{E}} \setminus \Sigma_{\mathcal{E}}$. To overcome this difficulty we may of course use the ε-approximations of Section 7.1:

$$[\mathbf{u} \text{ REL } \mathbf{v}]_{\mathcal{E}}^\varepsilon = [\mathbf{u} \text{ REL } \mathbf{v}]_{\mathcal{E}} \cap \{\mathbf{u} \,|\, (u_i^\alpha, u_{i+1}^\alpha) \in D_{i,\varepsilon} \text{ for } i = 0 \dots d-1 \text{ and } \alpha = 1 \dots n\}.$$

Now the flow is well-defined on the whole boundary $\partial[\mathbf{u} \text{ REL } \mathbf{v}]_{\mathcal{E}}^\varepsilon$.

As an example, let us suppose (u_k, u_{k+1}) is close to the northwest boundary $\overline{h^+}$ of D_k, say $u_{k+1} = h_\varepsilon^+(u_k)$ and $\varepsilon \to 0$. If all other pairs of coordinates (u_i, u_{i+1}), $i \neq k$ are not close

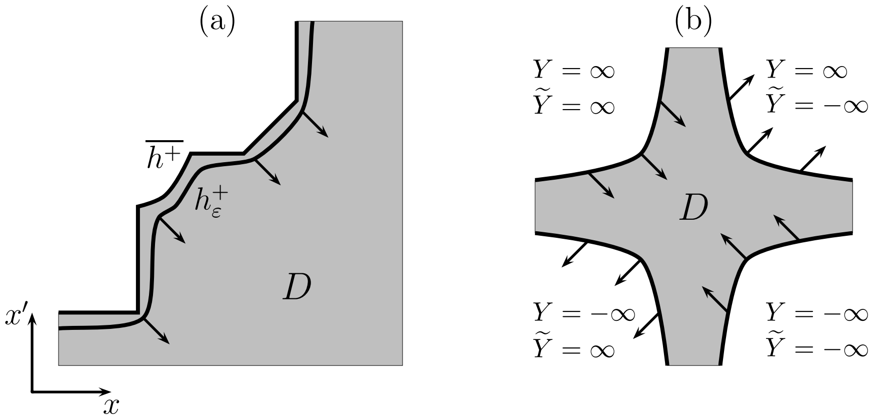

FIGURE 14. (a) The northwest corner and its ε-approximation with the direction of the flow. (b) Cartoon of the four pieces of boundary of the domain.

to the boundary, then, by (14), we have for sufficiently small ε that

$$\begin{aligned} \frac{du_k}{dt} &= Y_k(u_k, u_{k+1}) - \widetilde{Y}_{k-1}(u_{k-1}, u_k) > 0, \\ \frac{du_{k+1}}{dt} &= Y_{k+1}(u_{k+1}, u_{k+2}) - \widetilde{Y}_k(u_k, u_{k+1}) < 0. \end{aligned} \tag{15}$$

Since $h'_\varepsilon > 0$ the flow is thus directed inwards at this point, see Figure 14a. On the other boundaries similar arguments hold, which leads to the (mental) picture in Figure 14b.

However, we may have a problem when for example (u_{k-1}, u_k) also approaches a boundary. If it approaches the southeast or northeast boundary then there is no problem, since then $\widetilde{Y}_{k-1}(u_{k-1}, u_k) < 0$ and (15) still holds. On the other hand, if (u_{k-1}, u_k) approaches the northwest or southwest boundary then the two terms in (15) do not cooperate and we can draw no conclusion about the sign. In that case we are unable to conclude that $[\mathbf{u} \text{ REL } \mathbf{v}]^\varepsilon_E$ is isolating for the parabolic flow. We therefore need to introduce the notion of cooperation.

DEFINITION 7.1. A restricted relative braid class $[\mathbf{u} \text{ REL } \mathbf{v}]_\mathcal{E}$ is *cooperating*, if for any braid $\mathbf{u}$ in the boundary piece $\partial[\mathbf{u} \text{ REL } \mathbf{v}]_\mathcal{E} \setminus \Sigma_\mathcal{E}$, the following holds:

(1) if $(u_i^\alpha, u_{i+1}^\alpha) \in \overline{h_i^\pm}$, then $(u_{i-1}^\alpha, u_i^\alpha) \notin \overline{h_{i-1}^+} \cup \overline{g_{i-1}^-}$;
(2) if $(u_i^\alpha, u_{i+1}^\alpha) \in \overline{g_i^\pm}$, then $(u_{i-1}^\alpha, u_i^\alpha) \notin \overline{h_{i-1}^-} \cup \overline{g_{i-1}^+}$.

We want to link the index of the restricted braid class to that of the unrestricted braid class. For that purpose we need a stronger assumption, that also takes points in $[\mathbf{u} \text{ REL } \mathbf{v}] \setminus [\mathbf{u} \text{ REL } \mathbf{v}]_\mathcal{E}$ into account.

DEFINITION 7.2. A restricted relative braid class $[\mathbf{u} \text{ REL } \mathbf{v}]_{\mathcal{E}}$ is *strongly* cooperating if for any $\mathbf{u} \in \mathrm{cl}([\mathbf{u} \text{ REL } \mathbf{v}])$ the following holds:

(1) if $u_{i+1}^{\alpha} \geq h_i^{\pm}(u_i^{\alpha})$, then $u_i^{\alpha} < h_{i-1}^{+}(u_{i-1}^{\alpha})$ and $u_i^{\alpha} > g_{i-1}^{-}(u_{i-1}^{\alpha})$;
(2) if $u_{i+1}^{\alpha} \leq g_i^{\pm}(u_i^{\alpha})$, then $u_i^{\alpha} < h_{i-1}^{-}(u_{i-1}^{\alpha})$ and $u_i^{\alpha} > g_{i-1}^{+}(u_{i-1}^{\alpha})$.

We are now ready to state the main result. The statement and proof are similar to Section 8.3 in [**15**], where the restrictions on the domain were simpler and cooperation was automatic.

THEOREM 7.3. *Let $[\mathbf{u} \text{ REL } \mathbf{v}]_{\mathcal{E}}$ be a cooperating restricted braid class and let the unrestricted braid class $[\mathbf{u} \text{ REL } \mathbf{v}]$ be bounded and proper.*

(a) *Then the ε-approximation $N_\varepsilon = \mathrm{cl}([\mathbf{u} \text{ REL } \mathbf{v}]_{\mathcal{E}}^{\varepsilon})$ is an isolating neighborhood for the parabolic flow for all sufficiently small ε, which yields a well-defined Conley index, denoted by $h(\mathbf{u} \text{ REL } \mathbf{v}, \mathcal{E})$.*
(b) *Moreover, if $[\mathbf{u} \text{ REL } \mathbf{v}]_{\mathcal{E}}$ is strongly cooperating, then the index of the restricted braid class is the same as that of the unrestricted braid class: $h(\mathbf{u} \text{ REL } \mathbf{v}, \mathcal{E}) = h(\mathbf{u} \text{ REL } \mathbf{v})$.*

PROOF. Denote by $\widetilde{\mathcal{R}}_i$ the parabolic recurrence relation under consideration, with parabolic flow $\widetilde{\psi}^t$ defined on N_ε for all small ε. We first need to show that N_ε is isolating for sufficiently small ε. For any point $\mathbf{u} \in \partial N_\varepsilon \cap \Sigma_{\mathcal{E}}$ the flow $\widetilde{\psi}^t$ leaves N_ε in forward or backward time by Proposition 3.4. For any point $\mathbf{u} \in \partial N_\varepsilon \setminus \Sigma_{\mathcal{E}}$ the flow $\widetilde{\psi}^t$ leaves N_ε in forward or backward direction by the definition of a cooperating braid class and the arguments that lead up to its Definition 7.2. We thus conclude that N_ε is isolating, hence its Conley index is well-defined and is independent of (sufficiently small) ε.

Next consider the unrestricted braid class $[\mathbf{u} \text{ REL } \mathbf{v}]$. There exists a parabolic flow that fixes $\mathbf{v}$ (see Appendix of [**15**]), given by a recurrence relation $\mathcal{R}^0$ defined on $\mathbb{R}^3$. We are going to change the recurrence relation so that it still fixes $\mathbf{v}$, while the invariant set is guaranteed to be in the smaller set $[\mathbf{u} \text{ REL } \mathbf{v}]_{\mathcal{E}}$. Clearly $\mathbf{v} \in \mathcal{E}$ and also $\mathbf{v} \in \mathcal{E}_{2\varepsilon}$ for sufficiently small ε. Let $\eta \in C^\infty(\mathbb{R})$ such that $\eta(x) = 0$ for $x \leq 0$ and $\eta(x) = Ke^{-1/x}$ for $x > 0$, with large K to be chosen later. We construct a nonnegative function $\zeta_i(x, x')$ that is 0 on $D_{i,2\varepsilon}$ and that is large in some sense (see below) on the complement of the slightly larger $D_{i,\varepsilon}$. Namely, we define

$$\zeta_i(x,x') = \eta\big(x' - h^+_{i,2\varepsilon}(x)\big) + \eta\big(x' - h^-_{i,2\varepsilon}(x)\big) - \eta\big(g^+_{i,2\varepsilon}(x) - x'\big) - \eta\big(g^-_{i,2\varepsilon}(x) - x'\big);$$
$$\xi_i(x,x') = \eta\big(x' - h^+_{i,2\varepsilon}(x)\big) - \eta\big(x' - h^-_{i,2\varepsilon}(x)\big) - \eta\big(g^+_{i,2\varepsilon}(x) - x'\big) + \eta\big(g^-_{i,2\varepsilon}(x) - x'\big).$$

It is important that $\partial_2\zeta_i \geq 0$ and $\partial_1\xi_i \leq 0$ (they mirror the behavior of Y_i and $\widetilde{Y}_i$). For any large square N in $\mathbb{R}^2$ we can choose ε sufficiently small, so that the four terms have disjoint support in N. Additionally, for any $C > 0$ there is (by a straightforward compactness argument) a sufficiently large K so that

$$\zeta_i(x,x') = \eta(x' - h^{\pm}_{i,2\varepsilon}(x)) > C \qquad \text{on } N \cap \{x' \geq h^{\pm}_{i,\varepsilon}(x)\}; \tag{16a}$$
$$\zeta_i(x,x') = -\eta(g^{\pm}_{i,2\varepsilon}(x) - x') < -C \qquad \text{on } N \cap \{x' \leq g^{\pm}_{i,\varepsilon}(x)\}; \tag{16b}$$
$$\xi_i(x,x') = \pm\eta(x' - h^{\pm}_{i,2\varepsilon}(x)) \gtrless \pm C \qquad \text{on } N \cap \{x' \geq h^{\pm}_{i,\varepsilon}(x)\}; \tag{16c}$$
$$\xi_i(x,x') = \mp\eta(g^{\pm}_{i,2\varepsilon}(x) - x') \lesseqgtr \mp C \qquad \text{on } N \cap \{x' \leq g^{\pm}_{i,\varepsilon}(x)\}. \tag{16d}$$

We define for $s \in [0,1]$

$$\mathcal{R}^s_i(x_{i-1},x_i,x_{i+1}) = \mathcal{R}^0_i(x_{i-1},x_i,x_{i+1}) + s\left[\zeta_i(x_i,x_{i+1}) - \xi_{i-1}(x_{i-1},x_i)\right].$$

Let ψ^t_s be the flow generated by $\mathcal{R}^s$. By computing $\partial_1\mathcal{R}^s_i$ and $\partial_3\mathcal{R}^s_i$, it is not difficult to check that $\mathcal{R}^s$ is a parabolic recurrence relation and ψ^t_s a parabolic flow for all $s \in [0,1]$. Since $\mathcal{R}^s = \mathcal{R}^0$ on $\mathcal{E}_{2\varepsilon}$ the whole family fixes $\mathbf{v}$. Since $[\mathbf{u}\ \text{REL}\ \mathbf{v}]$ is bounded it is contained in a large cube, say $(u^\alpha_i, u^\alpha_{i+1}) \in N$ for all i and α. Using the strongly cooperating property of $[\mathbf{u}\ \text{REL}\ \mathbf{v}]$ we can deduce from (16) that for sufficiently large K the recurrence relations $\mathcal{R}^1_i$ and $\mathcal{R}^1_{i+1}$ have fixed sign whenever $(x_i, x_{i+1}) \in N \setminus D_{i,\varepsilon}$, for example, $\mathcal{R}^1_i > 0$ and $\mathcal{R}^1_{i+1} < 0$ when $x_{i+1} \geq h^+_{i,\varepsilon}(x_i)$. This implies that in forward or backward time the orbit through such a point leaves N. Therefore the invariant set for ψ^t_1 in $[\mathbf{u}\ \text{REL}\ \mathbf{v}]$ is completely contained in $[\mathbf{u}\ \text{REL}\ \mathbf{v}]^\varepsilon_{\mathcal{E}}$.

We now use the fact that the Conley index is a property not only of an isolating neighborhood, but also of an invariant set. Let S be the invariant set of $[\mathbf{u}\ \text{REL}\ \mathbf{v}]$ under the flow ψ^t_1. Since $[\mathbf{u}\ \text{REL}\ \mathbf{v}]^\varepsilon_{\mathcal{E}}$ is also an isolating neighborhood of S for ψ^t_1, we see that the Conley indexes of $[\mathbf{u}\ \text{REL}\ \mathbf{v}]$ and $[\mathbf{u}\ \text{REL}\ \mathbf{v}]^\varepsilon_{\mathcal{E}}$ are the same, namely the index of S.

Finally, consider the flows given by the interpolating parabolic recurrence relations $(1-\lambda)\widetilde{\mathcal{R}} + \lambda\mathcal{R}^1$, $\lambda \in [0,1]$, with parabolic flow $\widetilde{\psi}^t_\lambda$. Note that $\widetilde{\psi}^t_0 = \widetilde{\psi}^t$ and $\widetilde{\psi}^t_1 = \psi^t_1$, and the whole family fixes $\mathbf{v}$. Furthermore, $[\mathbf{u} \text{ REL } \mathbf{v}]^{\varepsilon}_{\mathcal{E}}$ is an isolating neighborhood for $\widetilde{\psi}^t_\lambda$ for any $\lambda \in [0,1]$, since the signs of $\mathcal{R}^1_i$ and $\widetilde{\mathcal{R}}_i$ on the restricting boundaries are the same. Hence the Conley index does not change along the continuation from $\widetilde{\psi}^t$ to ψ^t_1:

$$h(\mathbf{u} \text{ REL } \mathbf{v}, \mathcal{E}) = h([\mathbf{u} \text{ REL } \mathbf{v}]^{\varepsilon}_{\mathcal{E}}, \widetilde{\psi}^t) = h([\mathbf{u} \text{ REL } \mathbf{v}]^{\varepsilon}_{\mathcal{E}}, \psi^t_1) = h([\mathbf{u} \text{ REL } \mathbf{v}], \psi^t_1) = h(\mathbf{u} \text{ REL } \mathbf{v}).$$

This finishes the proof. $\square$

7.3. Positive entropy for bijective twist diffeomorphisms. Let us apply the theory developed in the previous section to prove Theorem 1.2. We can try to emulate Section 5 up to the point where we need to calculate the Conley index, which is now replaced by the restricted index $h([\mathbf{u} \text{ REL } \mathbf{v}], \mathcal{E})$. We need to be sure that the restricted index is well-defined. The braid classes under consideration are bounded and proper, but they might not all be cooperating.

Let us look at the shape of the domains D_i. Since the skeleton $\mathbf{v}$ (cf. Figures 7 (right) and 10) consists of stationary points, it must be that $(v^\alpha_i, v^\alpha_{i+1}) \in D_i$ for $\alpha = 1,2,3,4$. These points are shown in Figure 15 for even and odd i. For each i the projection of the unrestricted braid class $[\mathbf{u} \text{ REL } \mathbf{v}]$ under consideration onto the (u_i, u_{i+1})-plane is one of the three blocks indicated in Figure 15. As a consequence of the fact that $(v^\alpha_i, v^\alpha_{i+1}) \in D_i$ and of our knowledge about the shape of the boundary ∂D_i, we see that the northeast and southwest boundary never come into play for any of the braid classes under consideration, see Figure 15 again.

According to the definition of cooperating braid classes we need to prevent that (u_{i-1}, u_i) and (u_i, u_{i+1}) can be both on the northeast or both on the southwest boundary. When one retraces the steps, in particular the application of a flip in the proof of Lemma 5.1, one sees that this can only happen if in the associated symbol sequence -1 is adjacent to -1 or $+1$ is adjacent to $+1$, and we thus need to exclude these possibilities. To ensure the braid class is cooperating we therefore go back a step and replace the (full) shift on three symbols by a subshift with adjacency matrix

$$A = \begin{bmatrix} 0 & 1 & 1 \\ 1 & 1 & 1 \\ 1 & 1 & 0 \end{bmatrix}.$$

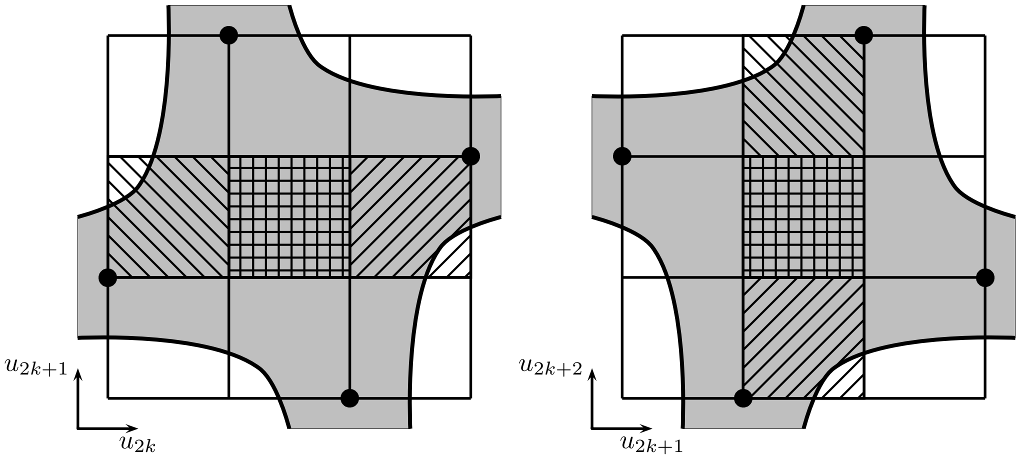

FIGURE 15. The dots represent the points $(v_i^\alpha, v_{i+1}^\alpha) \in D_i$, $\alpha = 1, 2, 3, 4$ for even i (left) and odd i (right). The domain D_i is indicated in gray. The projections of the unrestricted braid classes onto the (u_i, u_{i+1})-plane are hatched. Of the four boundaries of D_i only two can intersect the unrestricted braid classes.

In words, only sequences in which -1 is followed by 0 or $+1$, and $+1$ is followed by -1 or 0, are allowed. The corresponding braid classes are now all cooperating, and even strongly cooperating, so the remainder of the proof follows the path described in Section 5, using Theorem 7.3 to compute the restricted Conley index.

There is one more issue to deal with, namely compactness. The set Λ_1 as defined in (8) is not necessarily bounded, since, as should be clear at this point, it is harder to control the y-coordinates Y and $\widetilde{Y}$ for diffeomorphisms than it is for maps with the infinite twist condition. To resolve this problem, consider the set Λ_2 of periodic orbits of f^2 that is "constructed" in the same way as in Lemma 5.1 with the restriction on the symbol sequences due to the cooperating braid classes described above. To be more precise, for every symbol sequence in the subshift defined by A the proof of Lemma 5.1 gives a corresponding periodic point/orbit of f^2, and the collection of these orbits we call Λ_2.

Since Λ_2 consists of orbits it is invariant under f^2 and we claim that it is also bounded. Clearly the x-coordinates are uniformly bounded. The parameter ε, that is used to regularize in Section 7.1, can be chosen in a uniform manner, since there are only four different maps and four different domains $D_{i,\varepsilon}$ to consider. In the ε-approximations $[\mathbf{u} \text{ REL } \mathbf{v}]^\varepsilon_{\mathcal{E}}$ of the braid classes considered in Lemma 5.1, the pairs (x_i, x_{i+1}) are in a bounded subset of $D_{i,\varepsilon}$, and on these sets the continuous functions Y and $\widetilde{Y}$ are bounded. Hence also the y-coordinates of the points in Λ_2 are uniformly bounded.

The set Λ_1 in Section 5 is now replaced by the (smaller) compact set $\widetilde{\Lambda}_1 = \mathrm{cl}(\Lambda_2)$, which is invariant under f^2. Clearly this set $\widetilde{\Lambda}_1$ also suffices in Lemma 5.3, because that lemma essentially consists of taking the closure of the periodic trajectories. Replacing Λ_1 by $\widetilde{\Lambda}_1$ does not change any of the other arguments in Section 5. The resulting lower bound on the entropy of the bijective twist map is half of the entropy of the subshift, which is log of $1+\sqrt{2}$, the largest eigenvalue of the matrix A (cf. [**18**]).

References

1. S.B. Angenent, *The periodic orbits of an area preserving twist map*, Comm. Math. Phys. **115** (1988), 352–374.
2. ______, *Monotone recurrence relations, their birkhoff orbits and topological entropy*, Ergodic Theory Dynam. Systems **10** (1990), 15–41.
3. V.I. Arnold, *Mathematical methods of classical mechanics*, Graduate Texts in Math., vol. 60, Springer-Verlag, 1978.
4. S. Aubry and P.Y. Le Daeron, *The discrete Frenkel-Kontorova model and its extensions*, Physica D **8** (1983), 381–422.
5. J. Birman, *Braids, links and the mapping class group*, Ann. Math. Stud., vol. 82, Princeton Press, 1975.
6. P. Blanchard and J. Franks, *The dynamical complexity of orientation reversing homeomorphisms of surfaces*, Inv. Math. **62** (1980), 333–339.
7. P. Boyland, *An analog of Sharkovski's theorem for twist maps*, Hamiltonian dynamical systems, Contemp. Math., vol. 81, Amer. Math. Soc., 1988, pp. 119–133.
8. ______, *Topological methods in surface dynamics*, Topology Appl. **58** (1994), 223–298.
9. P.L. Boyland, H. Aref, and M.A. Stremler, *Topological fluid mechanics of stirring*, J. Fluid. Mech. **403** (2000), 277–304.
10. P. Le Calvez, *Propriétés dynamiques des difféomorphismes de l'anneau et du tore*, Astérisque (1991), no. 204.
11. C. Conley, *Isolated invariant sets and the morse index*, CBMS Regional Conference Series in Mathematics, vol. 38, AMS, 1978.
12. S. Day, O. Junge, and K. Mischaikow, *Towards automated chaos verification*, 2004, Preprint, To appear in Proc. Equadiff 2003.
13. W. de Melo and S.J. van Strien, *One-dimensional dynamics*, Springer-Verlag, 1993.

14. M. Dellnitz, G. Froyland, and O. Junge, *The algorithms behind GAIO – set oriented numerical methods for dynamical systems*, Ergodic theory, analysis, and efficient simulation of dynamical systems, Springer-Verlag, Berlin, 2001, pp. 145–174, 805–807.
15. R.W. Ghrist, J.B. van den Berg, and R.C. Vandervorst, *Morse theory on spaces of braids and Lagrangian dynamics*, Invent. Math. **152** (2003), 369–432.
16. M. Handel, *Orientation reversing homemorphisms of surfaces*, Topology **21** (1982), 291–296.
17. M. Hurley, *Noncompact chain recurrence and attraction*, Proc. Amer. Math. Soc. **115** (1992), 1139–1148.
18. B.P. Kitchens, *Symbolic dynamics*, Springer-Verlag, 1998.
19. T.Y. Li and J.A. Yorke, *Period three implies chaos*, Amer. Math. Monthly **82** (1975), 985–992.
20. J.N. Mather, *Existence of quasiperiodic orbits for twist homeomorphisms of the annulus*, Topology **21** (1982), 457–467.
21. K. Mischaikow, *Conley index theory*, Dynamical systems (Montecatini Terme, 1994), Lecture Notes in Math., vol. 1609, Springer-Verlag, 1995, pp. 119–207.
22. J. Moser, *On invariant curves of area-preserving mappings of an annulus*, Nachr. Akad. Wiss. Göttingen Math.-Phys. Kl. II **1962** (1962), 1–20.
23. ______, *Monotone twist mappings and the calculus of variations*, Ergodic Theory Dynam. Systems **6** (1986), 401–413.
24. C. Robinson, *Dynamical systems : stability, symbolic dynamics, and chaos*, 2nd ed., CRC Press, 1999.
25. A.N. Sharkowskii, *Coexistence of cycles of a continuous map of a line into itself*, Ukranian Math. J. **16** (1964), 61–71.
26. W.P. Thurston, *On the geometry and dynamics of diffeomorphisms of surfaces*, Bull. Amer. Math. Soc. **19** (1988), 417–431.

Department of Mathematics, Vrije Universiteit Amsterdam, De Boelelaan 1081, 1081 HV Amsterdam, the Netherlands.

E-mail address: `janbouwe@few.vu.nl, vdvorst@few.vu.nl, wwojcik@few.vu.nl`